Investeşte în oameni !
FONDUL SOCIAL EUROPEAN
Proiect cofinanţat din Fondul Social European prin Programul Operaţional Sectorial
Dezvoltarea Resurselor Umane 2007-2013
Axa prioritară 1: „Educaţia şi formarea profesională în sprijinul creşterii economice şi dezvoltării societăţii bazate pe cunoaştere”
Domeniul major de intervenţie 1.5 "Programe doctorale şi post-doctorale în sprijinul cercetării"
Titlul proiectului: „ Performanţă sustenabilă în cercetarea doctorală şi post doctorală-PERFORM”
Contract no. POSDRU/159/1.5/S/138963
Beneficiar: Universitatea Dunărea de Jos din Galaţi
Partener: Universitatea Ștefan cel Mare din Suceava

Ing. Alin-Mihai CĂILEAN

Referat 2

CONSIDERAŢII ASUPRA TEHNICILOR DE CODARE ŞI MODELAREA COMUNICAŢIILOR PRIN LUMINĂ VIZIBILĂ

(CONSIDERATIONS ON THE CODING TECHNIQUES AND VISIBLE LIGHT COMMUNICATION MODELING)

Coordonatori ştiinţifici,
Prof. univ. dr. ing. **Valentin POPA**
Prof. univ. dr. ing. **Luc CHASSAGNE**

Investeşte în oameni !

FONDUL SOCIAL EUROPEAN

Proiect cofinanţat din Fondul Social European prin Programul Operaţional Sectorial

Dezvoltarea Resurselor Umane 2007-2013

Această lucrare a beneficiat de suport financiar prin proiectul

Performanţă sustenabilă în cercetarea doctorală şi post doctorală-PERFORM

Contract no. POSDRU/159/1.5/S/138963

Proiect cofinanţat din Fondul Social European prin Programul Operaţional Sectorial Dezvoltarea Resurselor Umane 2007-2013

Table of contents:

List of figures:

List of abbreviations:

ADC	Analog to Digital Converter
AWGN	Additive White Gaussian Noise
ASCII	American Standard Code for Information Interchange
AGC	Automatic Gain Control
BER	Bit Error Ratio
DC	Direct Current
DD	Direct Detection
DMT	Discrete Multi-tone Modulations
DOT	Department Of Transportation
DSP	Digital Signal Processing
DSSS	Direct Sequence Spread Spectrum
FDM	Frequency Division Multiplexing
FOV	Field of View
FPGA	Field Programmable Gate Array
HPA	Half Power Angle
IEEE	Institute of Electrical and Electronic Engineers
IM	Intensity Modulation
IR	Infrared
ITS	Intelligent Transportation System
I2V	Infrastructure to Vehicle
LED	Lighting Emitting Diode
LoS	Line of Sight
MAC	Medium Access Control
MCS	Modulation and Codding Scheme
MFTP	Maximum Flickering Time Period
ML	Message Length
MIMO	Multi Input Multi Output
NRZ	Not Return to Zero
OFDM	Orthogonal Frequency Division Multiplexing

OOK	On Off Keying
PHY	Physical Layer
PWM	Pulse Width Modulation
PN	Pseudo Noise
PWM	Pulse Width Modulation
PSD	Power Spectral Density
RLL	Run Length Limiting
RSU	Road Side Unit
RF	Radio Frequency
SIK	Sequence Inverse Keying
SNR	Signal to Noise Ratio
VANET	Vehicular Ad-hoc Networks
V2V	Vehicle-to-Vehicle
VLC	Visible Light Communications
VPPM	Variable Pulse Position Modulation

1.1 Introduction

Nowadays, the modern society presents a growing demand for wireless communications technologies. This demand is encountered in more and more application fields. Such an application area is the Intelligent Transportation System (ITS). ITS plans to use the wireless data transfer for the so called communications-based safety applications. In these applications, wireless technologies are used to enable Vehicle-to-Vehicle (V2V) and Infrastructure-to-Vehicle (I2V) communications with the purpose of increasing the safety and the efficiency of the transportation system. Even if for many years, the radio frequency (RF) based solution were considered the dominating wireless communication technology, in the recent years, VLC came as an emerging alternative technology that could be more appropriate in certain scenarios. Such a scenario is encountered in a high traffic density area, where the increased number of notes that are using the communication medium leads to increased latencies [1, 2], which are unacceptable in traffic safety applications.

Due to numerous advantages, LED lighting systems began to be used in a lot of applications. Besides lighting, LEDs can enable VLC. VLC comes with several advantages and with plenty of challenges. VLC is safe for the human health unlike radiofrequency waves which are considered as possibly cancerous to humans [3] or like infrared communications which can cause thermal damage on the cornea. VLC also offers worldwide unregulated unlimited bandwidth, having the potential for extremely high data rates that can go above 1 Gbps [4].

One particular application area for the VLC, is in the Intelligent Transportation System (ITS), where it can be used for Infrastructure-to-Vehicle (I2V) [5, 6], and for Vehicle-to-Vehicle (V2V) [7, 8] communications. Enabling inter-vehicle communication has the potential to substantially improve the safety and the efficiency of the transportation system, addressing up to 81 percent of all-vehicle crashes [9].

In the recent years, LED-based lighting has begun to be integrated in the transportation system. The car manufactures began to replace the halogen lamps by LEDs, whereas city authorities use LEDs systems to replace the classical street lighting systems and integrate them in traffic lights. This enables VLC to be a ubiquitous technology, capable to ensure a high market penetration, contributing to the success of the ITS.

The usage of VLC for transportation related applications was first considered in 1998 [10, 11], and since then much effort has been made on this topic. Numerous communication systems that use VLC for I2V [12, 13] or for V2V [7, 14] communication have been developed and proved their reliability. Regarding the requirements imposed for the Vehicular Ad-hoc Networks (VANET) [15], VLC is considered to be able to satisfy them even in real working conditions [16]. Even if the communication range of these systems is not as high as for those using RF solutions, multi-hop VLC has proven that by combining short and medium range communications the overall communication distance can be increased [17]. At this point, VLC usage for transportation related application involves relatively low data rates of kbps or of few Mbps.

This research activity report presents an analysis of the Miller coding technique and of its appropriateness for VLC outdoor usage in ITS application comparing it with the Manchester code. Simulation results show that in terms of bandwidth and channel coexistence the Miller code clearly outperforms the Manchester code, whereas the results confirm that in terms of BER, both the codes have similar performances. Since the IEEE 802.15.7 [18] standard, choses the usage of the Manchester code taking into consideration its flickering performances, an analysis on the flickering performances of the Miller code is also performed. This is the first detailed analysis that focuses on the Miller code VLC potential usage.

This research activity report also presents the simulation and experimental results concerning the negative effects of noise on the received data signal, specially focusing on the pulse width distortions. The analysis is performed on messages coded using the Manchester and the Miller code. The simulations were carried based on a signal that was digitally processed, whereas the experimental tests were conducted using a signal processed mostly in an analogical manner, on a VLC receiver [19]. This is also the first work that approaches the issues concerning the noise effect on VLC at the pulse level, investigating the distortion it produces.

This research activity report presents theoretical simulations and experimental contributions related with the outdoor VLC. It analyses the performances of the Manchester coding and proposes the usage of the Miller code. The report analyses the two codes from several perspectives. Simulation results and experimental tests are provided.

1.2 The IEEE 802.15.7 Standard for Short-Range Wireless Optical Communication using Visible Light

The IEEE 802.15.7 draft standard for short-range wireless optical communication using visible light had become available in 2011. The standard states that the VLC data transfer is achieved using intensity modulation of optical devices such as LEDs at frequencies imperceptible for the human eye. The standard covers the physical layer (PHY) and the medium-access control (MAC). Currently the MAC supports three access topologies: peer-to-peer, star, and broadcast.

The IEEE 802.15.7 standard comes with three PHY types grouped by data rates and by the intended applications. PHY 1 is intended for outdoor low data rate applications and it uses on-off-keying (OOK) and variable pulse position modulation (VPPM). This mode has specified data rates between 11.67 and 267 kb/s. For the OOK, the standard specifies Manchester code as the code to be used whereas for forward error correction, Convolutional and Reed Solomon codes can be used. PHY 2 is intended for indoor moderate data rate applications and it also uses OOK and VPPM. For this mode date rates between 1.25 and 96 Mb/s are specified. For forward error correction Reed Solomon codes can be used. PHY 3 is intended for color-shift-keying applications with data rates between 1.25 and 96 Mb/s. Again, Reed Solomon codes can be used for error correction. The three PHY types can coexist but are not able to interoperate. PHY I occupies different spectral regions in the modulation spectrum from PHY II or PHY III. As shown in Fig. 1.1, this enables frequency division multiplexing (FDM) as a coexistence technique.

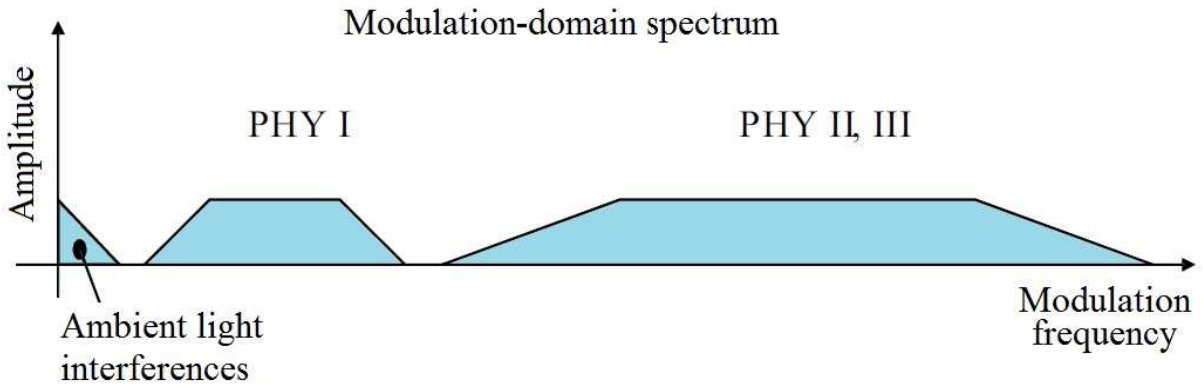

Fig.1.1: Frequency Division Multiplexing of the three PHY types.

The standard considers the issues related with the mobility of the link, the impairments caused by noise and interference from other light sources. Unlike other wireless communication technologies, in VLC the light wave carrier is perceivable for the human eye. This imposes that the modulation process must not cause any noticeable flickering that might affect the human health. Another unique feature of VLC is the requirement for supporting communications while light source dimming. These two aspects are taken into consideration by the standard, imposing strict limits for flickering and high resolution diming.

The standard considers as a possible application field the ITS domain, for communication between vehicles and also with the traffic infrastructure defining several of the aspects related with the networking and the requirements imposed in this application field. The inclusion on the ITS applications in the IEEE 802.15.7 standard is an encouraging factor for continuing the research in this domain.

2. Considerations regarding the coding techniques used for VLC

2.1 Introduction

In general, Intensity Modulation (IM) is considered to be the most appropriate modulation technique for VLC. IM implies modulating the desired waveform onto the instantaneous power of the carrier. The receiver extracts the data from the modulated light beam by using Direct Detection (DD). The photodetector generates an electrical current proportional to the incident power. This current is further transformed into a voltage by a transimpedance circuit and then the signal passes through several filtering and amplification stages until the data signal is reconstructed.

Depending on the application, many modulations techniques were proposed and investigated for VLC usage. Orthogonal Frequency Division Multiplexing (OFDM) [20] and discrete multi-tone modulations (DMT) [21] techniques offer the premises for high data rates and are used mainly for indoor static applications. But, high complexity modulations are to the detriment of the usage of an increased complexity transceiver. For applications that require dimming, Pulse Width Modulation (PWM) [22] is considered an alternative. For low data rates applications meant for outdoor usage, where the Signal-to-Noise Ratio (SNR) is low, simpler modulations techniques are generally used. OOK is a simple solution that proved to be quite

efficient. OOK modulation is regularly used with Not Return to Zero (NRZ) or with Manchester coding. The usage of Pulse Position Modulation (PPM) or of Inverted-PPM [23], have also been investigated. Compared with OOK, PPM and I-PPM can achieve higher data rates but require more bandwidth, higher peak power and are more sensitive to noise. In order to reduce the effect of noise, the usage of Direct Sequence Spread Spectrum (DSSS) sequence inverse keying (SIK) has been investigated and implemented [5, 13]. This approach uses a pseudo noise (PN) sequence that is used to encode the bit '1', whereas for bit '0' it uses its complement. This type of coding has error detecting capabilities and enables multiple transmitters.

The IEEE 802.15.7 standard for wireless optical communications using visible light defines for the PHY I outdoor usage, the utilization of OOK and of Variable Pulse Position Modulation (VPPM) as possible modulation techniques. VPPM is an improved modulation technique that combines the characteristics of pulse position modulation (2-PPM) for non-flicker and of Pulse Width Modulation (PWM) for dimming control and brightness control. VPPM is similar to 2-PPM but it allows the pulse width to be controlled, for light dimming. All VPPM PHY I modes use 4B6B encoding. The 4B6B code is a simple data transmission code. The description of the block code is done based on a coding table which contains the output codes associated with the input codes. The code involves series of '0' and '1' pulses. The 4B6B code expands every 4 bits in to 6 bits, with the number of 1s equal with the number of 0s. VPPM is intended mostly for applications that require dimming, which is not the case of a traffic light. However, VPPM could be used to enable I2V communication between street lighting infrastructure and vehicles where light intensity control applications with the purpose of reducing the energy consumption which is also a hot topic [24, 25]. For application where the light intensity is constant and where no dimming is required, like the applications related with the V2V communication or the communication between a traffic light and a vehicle, OOK is considered more appropriate.

2.2 OOK coding techniques

OOK is a simple modulation technique in which the digital data is represented as the presence of the signal, corresponding to the "ON" state whereas the absence of the data is represented as the absence of the signal, or the "OFF" state. The "ON" and the "OFF" represent two distinct amplitude levels, required for the purpose of communication and not necessarily

imply that the light source is turned OFF completely. For OOK, the IEEE 802.15.7 standard mentions the usage of the Manchester code, with five different data rates, namely 11.67, 24.44, 48.89, 73.3 and 100 kb/s.

2.2.1 Not-Return to Zero (NRZ)

NRZ is the simplest OOK coding. In this code a binary 1 is represented as a non-zero voltage level, whereas a binary 0 is represented by a zero voltage level. The NRZ code is not a self-synchronizing code, so for proper working it requires same additional synchronization technique.

The Power Spectral Density (PSD) of NRZ code is given by:

$$S_{NRZ}(f) = \frac{V^2 T}{4}\left(\frac{\sin \pi f T}{\pi f T}\right)^2 + \frac{V^2}{4}\delta(f), \tag{2.1}$$

where V is the signal amplitude, $T=1/R$ is the bit duration, R is the bit rate in bits per second and f is the frequency for which the PSD is calculated.

NRZ is considered an easy to implement code but has the disadvantage of being strongly affected by interferences due to other light sources with or without transmitting capabilities. Another disadvantage of NRZ is the significant DC component and dc content. NRZ can also suffer from loss of synchronization for long sequences of 1s or 0s. The error performance rate of NRZ code is also one of its disadvantages. For equally likely data, with additive white Gaussian noise (AWGN) and optimum filter, is given by:

$$Pe = \frac{1}{2} erfc\left(\sqrt{\frac{E_b}{2N_0}}\right) \tag{2.2}$$

where E_b/N_0 is the signal-to-noise ratio (SNR) of the received signal.

Since outdoor long distance VLC is subject to numerous noise sources that significantly affect the SNR, NRZ is not considered appropriate for VLC.

2.2.2 Manchester code

Manchester coding is an instantaneous transition code developed by University of Manchester, in which each bit has at least one transition that occurs at the mid-bit position. This feature allows the recovering of the clock signal from the data frame. The DC component of the Manchester code is zero.

In Manchester coding, a binary "1" is represented by a high to low transition, whereas a binary "0" is represented by a low to high transition. Basically, each bit is expanded in an encoded 2 bit pair, and so, compared with NRZ, Manchester code requires twice the baseband bandwidth.

The Power Spectral Density (PSD) of Manchester code is given by eq. 3:

$$S_{Man}(f) = V^2 T \cdot \left[\left(\frac{\sin^2(\pi f T/2)}{\pi f T/2} \right) \right]^2 \tag{2.3}$$

IEEE Standard for Short-Range Wireless Optical Communication Using Visible Light, standard 802.15.7 specifies the use of Manchester coding for low data rate, outdoor usage of VLC. The standard specifies 5 possible data rates form 11.67 kb/s up to 100 kb/s. Besides the advantages mentioned above, another reason that made the Manchester code being considered by the upper mentioned standard is due to its flickering performances. In Manchester code, flickering is prevented by ensuring the same brightness for both "1" and "0" bits, since the positive pulses period is equal with the negative pulses period.

2.2.3 Delay Modulation (Miller code)

The Miller code [26] can be easily constructed from the Manchester code. The Miller code is also a transition code but with memory. In Miller code, "1" is represented by a transition on the mid-bit position, "0" is represented by no transition on the mid-bit position whereas "0" fallowed by "0" is represented by a transition at the end of the first 0's period. The Miller code offers good timing and also has the advantage that it requires a low bandwidth.

Even if the Miller code not as popular as the Manchester code, its evaluation is necessary since it could be convenient for further Multiple Input Multiple Output (MIMO) applications, since it uses the bandwidth more efficiently. Compared with the Manchester coding, its carrier

tracking is accomplished easier.

The Miller code behavior seems to be very suitable in order to perform multi-channels communication. The Power Spectral Density (PSD) of Miller code is given by eq. 3:

$$S_{Miller}(f) = \frac{V^2 T}{2(\pi\ f\ T)^2 \cdot [17 + 8\cos(2\pi\ f\ T)]} \cdot \begin{matrix} [23 - 2\cos(\pi\ f\ T) - 22\cos(2\pi\ f\ T) \\ -12\cos(3\pi\ f\ T) + 5\cos(4\pi\ f\ T) \\ +12\cos(5\pi\ f\ T) + 2\cos(6\pi\ f\ T) \\ -8\cos(7\pi\ f\ T) + 2\cos(7\pi\ f\ T)] \end{matrix} \quad (2.4)$$

2.3 Comparative evaluation of Manchester and Miller code

Based on the fact that in the case of outdoor low data rate applications, such as those between vehicles or those between traffic infrastructure and vehicles, the Manchester code is stated in the IEEE 802.15.7 standard makes it a leading code for such VLC applications. Under these conditions, further investigation and evaluation of the Manchester code is strongly imposed.

However, in the context of a strong requirement for MIMO application, the investigation of a code suited for such applications is also required. For this reason, the usage of the Miller code in VLC under the PHY I layer of the IEEE 802.15.7 standard is also investigated in parallel with the Manchester code usage.

This investigation will take into consideration several key points related to the code performances, such as:

- the multi-channel capabilities;
- the flickering performances;
- the sensitivity to noise;
- the error occurrence;
- the bit error ratio (BER).

2.3.1 Considerations on multi-channel capabilities for Manchester and Miller codes

The Manchester code, also called the biphase code, is a classical code, in which ‘0’ is encoded as ‘01’, whereas ‘1’ becomes ‘10’. This codding technique has numerous advantages

like DC balance, easy clock and data recovery, decent BER performances. However, even if it has plenty advantages, Manchester code's bandwidth requirements are larger than of any other common codes. For example, it requires twice the bandwidth of Not-Return to Zero (NRZ). On the other hand, the Miller code, also known as delay modulation, appears to be more convenient for Multiple Input Multiple Output (MIMO) applications, since it uses the bandwidth more efficient.

Even if the performances of the NRZ code are not addressed by this study, it has been introduced as a reference. The MATLAB simulation results containing the corresponding curves for a modulation frequency of 11.67 kHz are plotted in Fig. 2.1. It can be noticed that the Manchester code requires twice the bandwidth of the NRZ code. For the Miller code's PSD, the maximum energy is at a frequency of around 2/5 of the modulation frequency. Fig. 2.2 and Fig. 2.3 illustrate the MATLAB simulation results containing the coexistence of five adjacent channels for the data rates specified by the 802.11.7 standard for OOK, for Manchester and Miller codes respectively. It can be obseved that for Manchester code, the five carriers overlap, making the separation quite difficult and introducing decoding errors. In the case of the Miller code, the five channels can be well distinguished. This allows for the five sub-carriers to be more easily filtered by band-pass filters, either analog or digital.

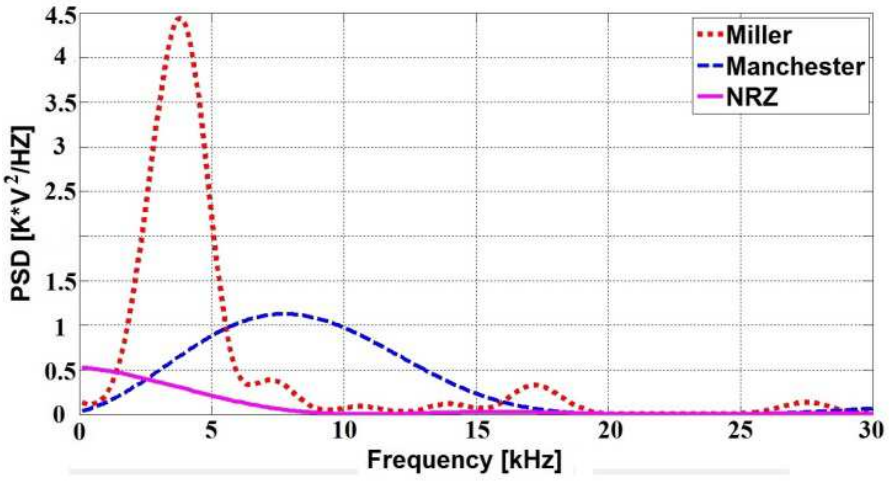

Fig. 2.1: PSD for NRZ, Manchester and Miller code at 11.67 kHz.

The Miller code can be easily constructed using the Manchester code. In Miller code, a '1' is encoded as a transition on the mid-bit position, a '0' following a '1' is encoded as no

transition on the entire bit period, whereas a ‘0’ following a ‘0’ is encoded as a transition on the beginning of the second bit period. The Miller code has very good timing content, and carrier tracking is easier than Manchester coding.

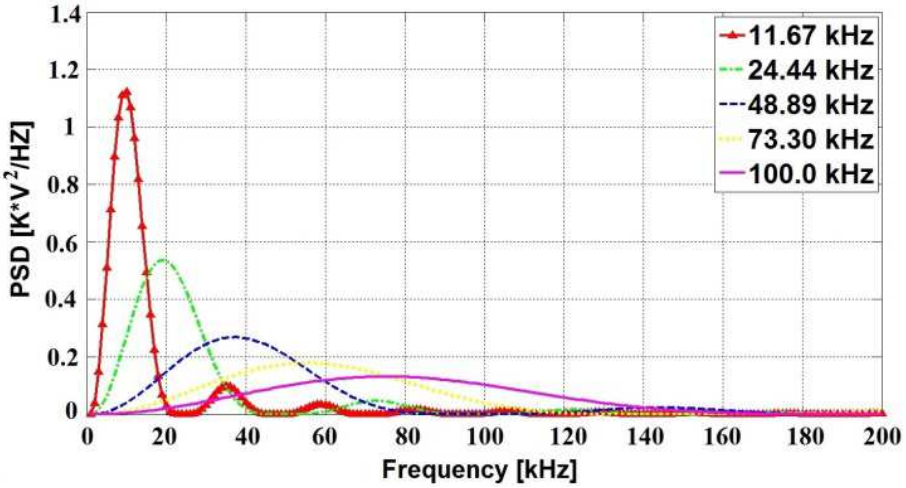

Fig. 2.2: Simulation for a five channels configuration, using the Manchester code.

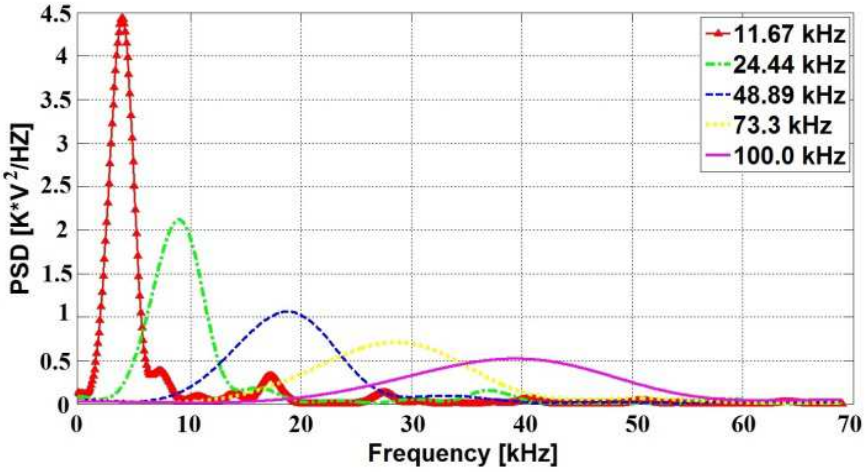

Fig. 2.3: Simulation for a five channels configuration, using the Miller code.

The curves are proportional to a scale factor K depending on the amplitude of the signal but nevertheless, the key point is the relative scale between curves.

2.3.2 Flickering issues concerning the Manchester and the Miller code

The VLC technology adds communication capabilities to the classical lighting. However,

VLC must not affect in either way the primary role of the appliance, which is lighting or signaling. Flickering mitigation is one of the main concerns regarding the VLC. Flickering represents the light intensity fluctuation caused by the modulation technique, and it is classified as inter-frame flickering and as intra-frame flickering. Flickering is prevented when the light intensity changes within the Maximum Flickering Time Period (MFTP). In this case the human eye does not notice the light intensity changes. Even if an optimal flicker frequency is not widely accepted, it is considered that a MFTP smaller than 5ms (200 Hz) is safe [18, 27]. The IEEE 802.15.7 standard specifies the usage of Run Length Limiting (RLL) line coding, such as Manchester, 4B6B or 8B10B code, as a technique for preventing perceivable flickering. The RLL codes prevent long runs of 1s and 0s that can cause flickering and also ensure better clock and data recovery. For outdoor usage, the IEEE 802.15.7 standard specifies for the OOK, the usage of Manchester as a technique for preventing perceivable flickering, whereas for VPPM, it specifies the usage of the 4B6B code. For both the modulations, the non-flickering characteristic is achieved by having the same brightness for bits “1” and “0”.

Due to its characteristics, the Miller code cannot ensure the same brightness for bits “1” and “0”. For bit “1”, every bit has the same brightness. But, for “0”, the brightness can be either twice the brightness of “1” or it can be zero. Under these considerations, instead of determining the brightness of Miller coded messages on an individual bit level, the determination is performed on a byte level. It seems that as long as the modulation period is at least eight of the MFTP, if each byte’s brightness is equal, no noticeable flickering is induced.

To determine the flickering characteristic of the Miller code several simulations MATLAB have been performed. A number of 10^5 messages, containing 64 random ASCII characters (512 bits) were generated. The messages were encoded using the Miller code. The brightness of each byte is determined by measuring the “lights on” time as a percentage of the total byte time. It is considered that 100% brightness is achieved when the light is on for half of the byte time (as for the Manchester code). The simulation results concerning the brightness intensity variations at the byte level are exposed in Fig. 2.4. It can be observed that the brightness of the bytes is 100% for 37.46% of the cases, varies in 49% of the cases by ±12.5%, in 12.5% of the cases by ±25%, whereas in 0.7% of the cases by ±37.5%.

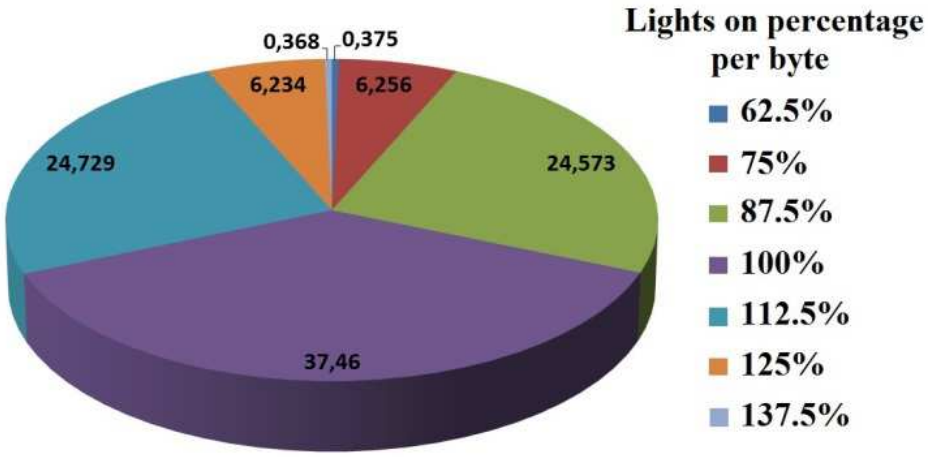

Fig. 2.4: Simulation results showing the bytes percentage for different brightness intensities.

Based on these results, one can conclude that unlike the Manchester code, the Miller code exhibits some brightness variations from one byte to another. However, since the byte period is significantly shorter than the MFTP, flickering at the byte level cannot be perceived. In the following step it will be determined the brightness of each MFTP, for the five data rates mentioned by the standard. The MATLAB simulation results are presented in Fig. 2.5. It can be observed that the MFTP's brightness has a Gaussian distribution, centered on the 100% brightness intensity, which gets narrower as the modulation frequency increases. The results show that even at the lowest data rate, more than 96% of the MFTPs have an oscillation bellow ±10%. Furthermore, the human eye does not have a linear response to changes in light intensity. According to [28], the relation between the perceived light and the measured light is given by eq. 1. This relation further reduces brightness variation sensation, limiting the flickering effect perceived by the human eye.

$$Perceived\ light(\%) = 100 \times \sqrt{\frac{Measures\ light(\%)}{100}} \tag{1}$$

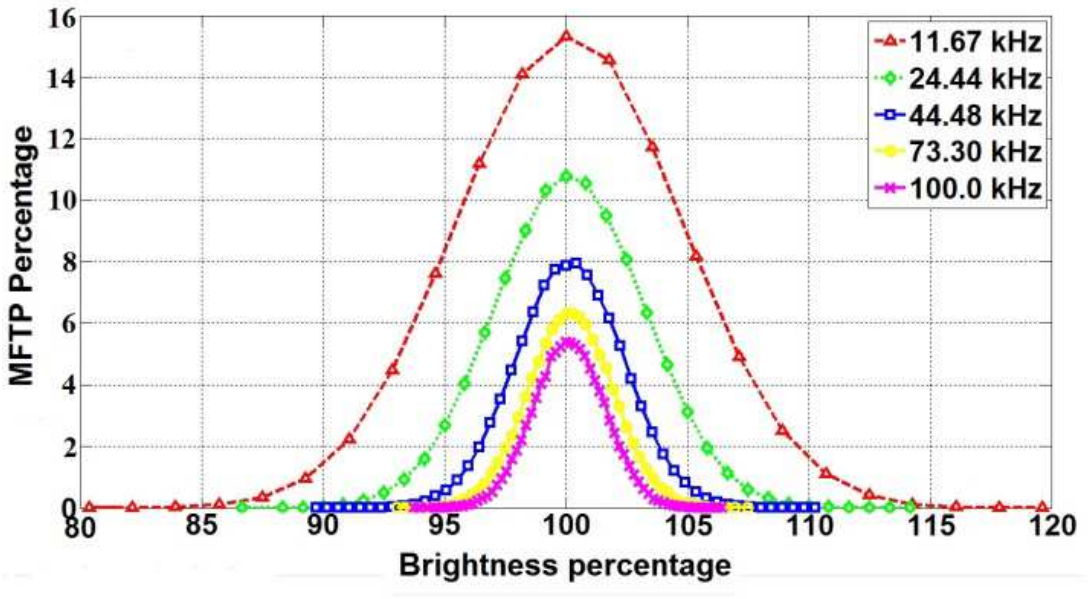

Fig. 2.5: Simulation results showing the percentage of MFTP for different brightness percentages.

2.3.3 Sensitivity to noise

IM with DD implies the usage of a photodetector element that produces the current proportional with the incident light. This current will be further processed in order to obtain the data it contains. However, the incident power not only contains the data signal but also noise. The outdoor VLC channel is considered to be extremely noisy. Sun light, street light and vehicle lighting systems represent major background noise sources for VLC. These high noise interferences are corroborated with low-level signals due to signal degradation over the distance. The weather conditions, such as fog or rain, also have a negative impact on the VLC data signal. More than that, due to the dynamic nature of the traffic, in such applications, the VLC receiver will experience high variations of the SNR. Of course, different mitigation mechanisms such as narrow angle receiver, optical filters, or different signal processing techniques are used at the receiver side, but still, high levels of noise will affect the quality of the communication. Therefore, an analysis of the effects of the noisy optical channel on the data signal is strongly needed.

In order to determine the noise influence on the pulse width, several MATLAB/Simulink

simulations have been performed. The simulations involve the coding of random messages using both the Manchester and the Miller code. The messages are transmitted using a modulation frequency of 15 kHz and at three different SNR levels. The receiver simulated assumes the use of a 12 bits ADC module. In order to be able to insure decent signal processing, the sampling frequency is 100 times the data frequency, leading to 1.5 MHz.

The filtering is performed by two low-pass Butterworth 2^{nd} order cascading filters separated by a partial signal reconstruction block. After filtering, the signal passes through a two level triggering block that outputs the replication of the emitted signal. The reconstructed message pulse widths are then measured and analyzed in order to determine the noise influence on the pulse widths. In this case, the simulated set up was a simplified version of the model described in Chapter 3. More complex signal processing techniques, higher order filtering or adaptive threshold algorithms can minimize the effect of the current noise levels, but as the SNR continues to depreciate the effects on the pulse widths are similar.

For the purpose of these experiments random messages were coded in Manchester and Miller code. The main parameter is the width of the elementary moments of the digital bits. For the Manchester code, there are only two symbols (positive edge and negative edge) and it leads statistically to only two combinations of widths: either one elementary bit width, either twice. For the Miller code, the memory effect on its construction leads to three possible combinations: either one momentary width, or one and a half or twice the widths [29]. The possible variations of the pulse widths for the two codes are presented in Fig. 2.6.

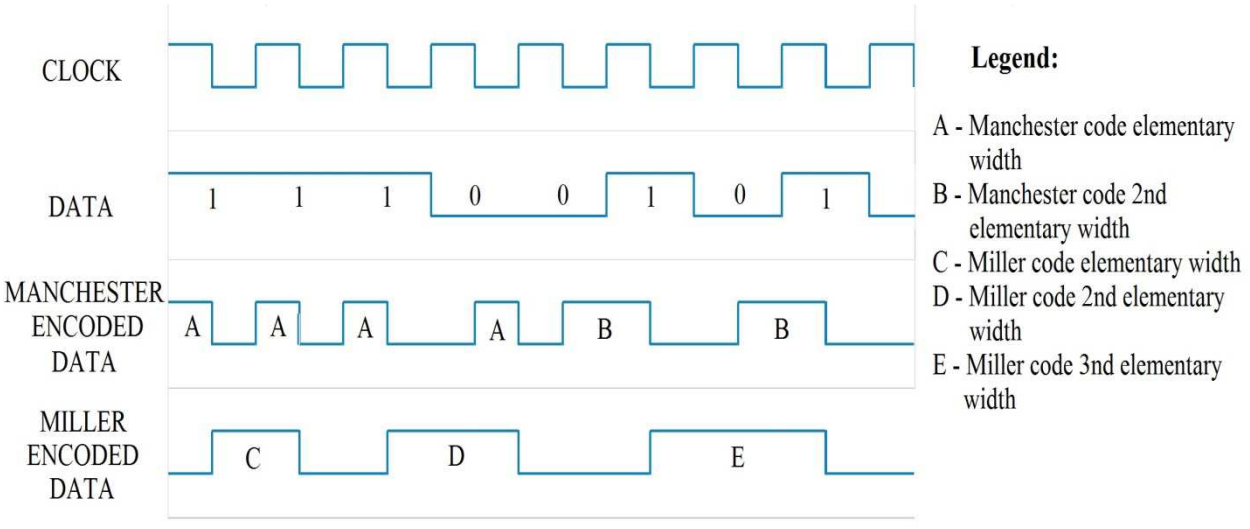

Fig. 2.6: Illustration of the possible pulse widths in Manchester and in Miller code

At the receiver side, after passing through the stages mentioned above, the values of 10^5 pulses from each of the pulse widths types were saved and then analyzed for both codes. It has to be mentioned that for both Manchester and Miller code, a coded frame does not contain equal numbers of pulses from the two respectively the three pulse widths types. The number of pulses from each category is depending of each message. From this reason the data gathering process continued until the 10^5 number of pulses from each of the pulse widths types was achieved.

Even if the purpose of this analysis is not message decoding, it is important to mention that decoding is performed based on the identification of the rising and falling edges and on the pulse width measurement. In this case it is obvious that pulse distortions above certain tolerances will cause decoding errors.

The results concerning the noise effects on the pulse width are plotted in figure 2.6 for three SNR levels for the Manchester and for the Miller code. It can be noticed that as the SNR decreases, the pulse widths are affected by distortion. Also, in the same time, the number of pulses that are affected is significantly increasing.

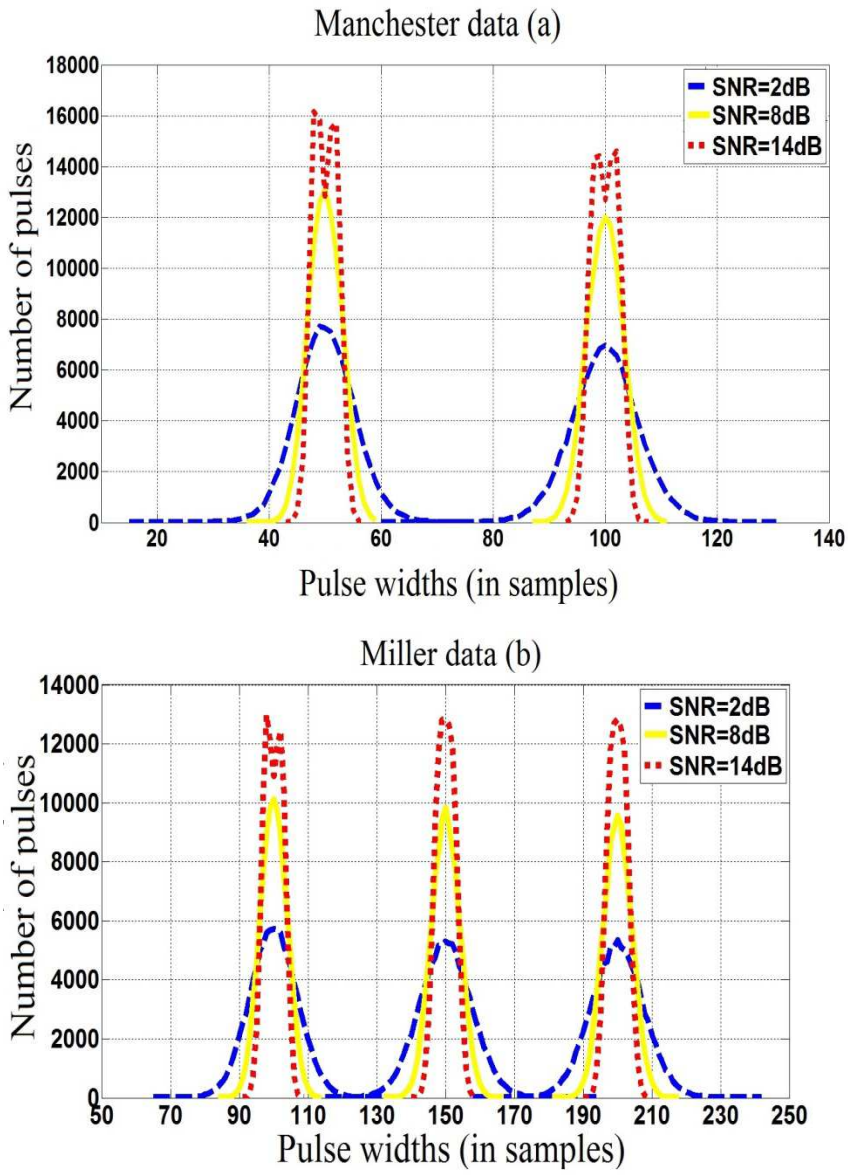

Fig. 2.7: Simulation results for Manchester and Miller code pulse widths: a) Manchester case b) Miller case

The pulse width distortions do not represent a significant problem as long as they do not affect the pulse width in a percent that is creating uncertainty for data decoding. It can be observed that in the case of the Miller code, the distortion percentage is not as high as for the Manchester code. This can be explained because due to its larger pulse width, it uses a greater number of samples per pulse, resulting into a better filtering. However, due to its nature, the Miller code is more sensitive to variation of pulse length. In its case, pulse width variations of

12.5 to 25% create uncertainty in decoding. In the case of the Manchester code, the distortion percentage that creates uncertainty is double.

Fig. 2.7 presents the number of pulses that were affected by distortion in a degree that induces decoding errors for both the two codes. It can be observed that in the case of the Miller code, the Pulse Error Rate (PER) is significantly higher than the PER of the Manchester code. However, a Miller pulse has a greater length and therefore it carries more data, making the Bit Error Ratio (BER) quite similar with the one of the Manchester code.

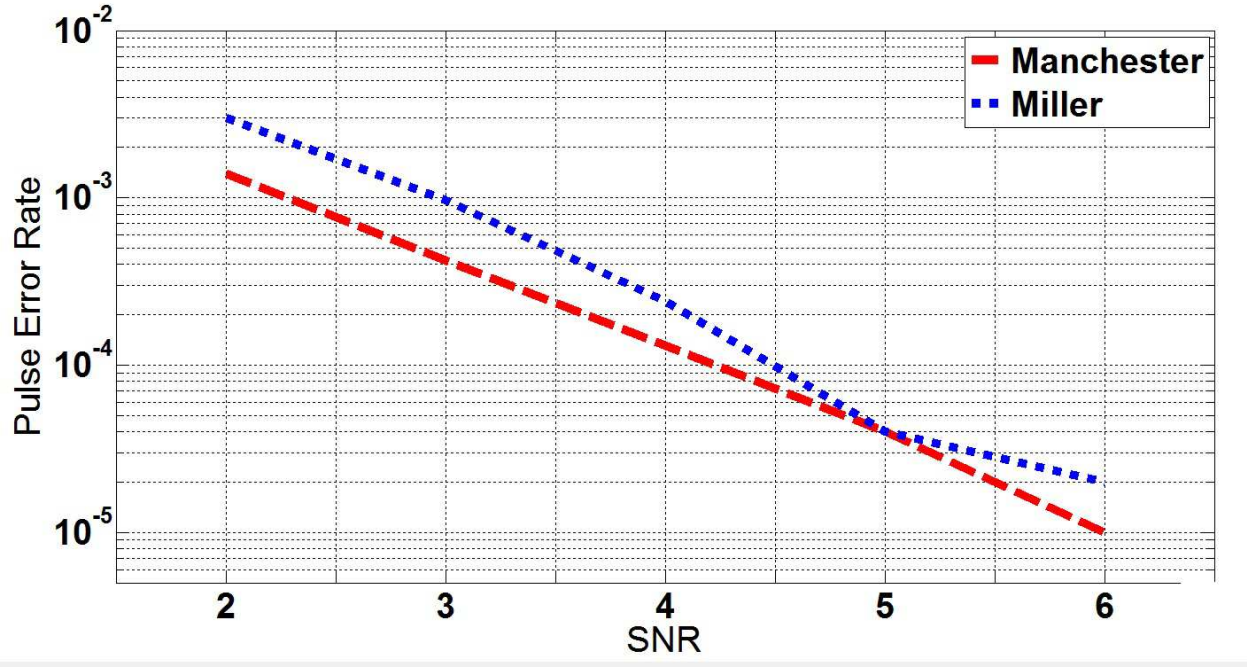

Fig. 2.8: Pulse error ratio for Manchester and for Miller codes

Another interesting finding revealed during these tests is related to the nature of the errors. In the case of the Manchester code more than 75% of the errors are due to missing of edges due to insufficient filtering. Basically, due to the noise and because of the limited number of samples per pulse used in the filtering, the signal quality was low and in those cases proper signal reconstruction was unachieved. On the other hand, in the case of the Miller code, the errors are due to the limited tolerances. For example, for a double length Miller pulse, a -12.5% distortion creates uncertainty in decoding with a middle size pulse.

Regarding the BER results, these are represented in Fig. 2.8. It can be noticed that at low SNR, the Miller code and the Manchester code present almost similar results with a 10% better BER in the case of the Miller code. However, as the SNR improves (4 – 5 dB), the BER

performances seem to get better in the case of the Manchester code, and tend to get even considering a 10^{-7} level.

This behavior can once again be attributed to the nature of the two codes. At low SNR levels, the improved filtering performances of the Miller code give it a slight advantage over the Manchester code. As the SNR gets higher, the Manchester coded signal is decently filtered while the Miller coded signal is affected by the stricter tolerance limit.

Of course, these results can be improved by using higher level filtering, improved pulse reconstruction algorithms or other signal processing techniques, that will mitigate the noise effects on the pulse width to lower SNR levels.

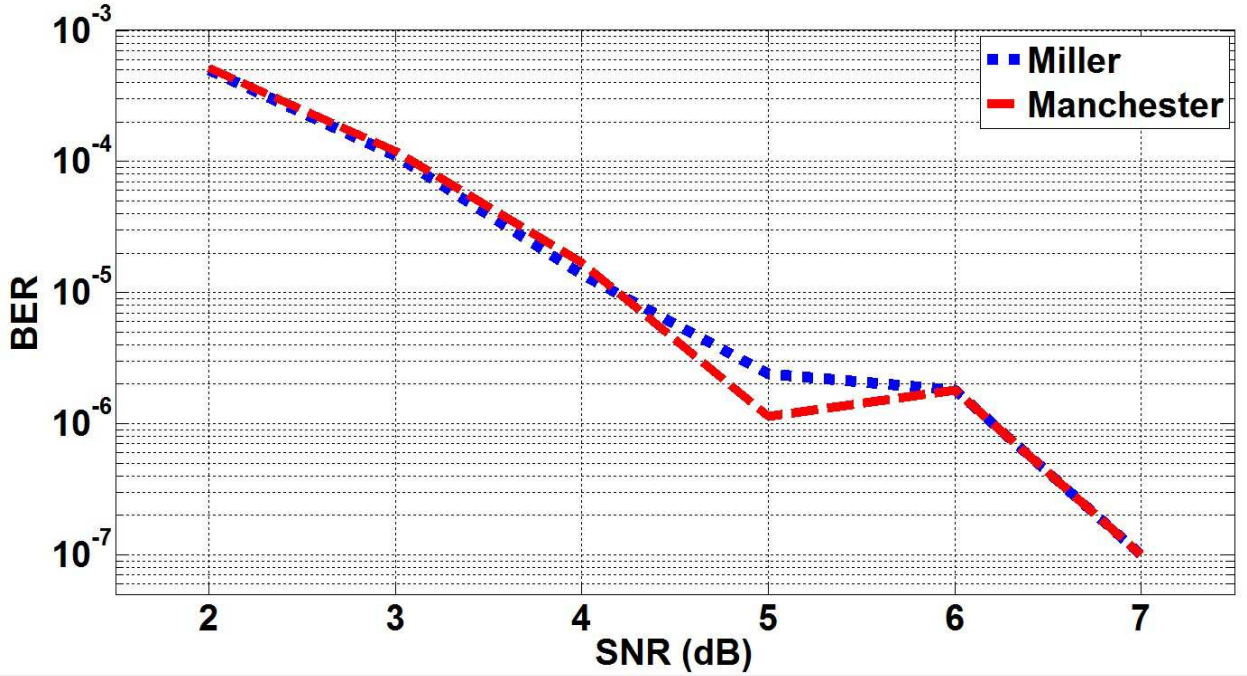

Fig. 2.9: Bit error ratio for Manchester and for Miller codes

2.3.4 Experimental results concerning the pulse width measurement

The experimental measurements of the pulse widths were determined by using a microcontroller based VLC receiver. More details regarding its architecture and its performances are provided in [30]. In this prototype, the microcontroller can be switched either on Manchester or Miller in order to test different configurations. For the detection board, the temporal properties

of both codes are important to design the electronics without using complex decoding algorithms which reduces hardware complexity and helps reducing the implementation costs.

The experimental tests were performed with a commercial traffic light (red and green lights) in indoor configurations, as presented in Fig. 2.9. The emitter and the receiver boards include low-cost microcontrollers. The emitter and the receiver are interfaced with a PC through a USB. Basically, the message transmitted during the experiments is sent to the emitter and the frame indicates if Miller or Manchester code is selected. The receiver decodes the data in real-time and an algorithm allows post-processing or calculation of errors.

For these experiments, a specific message is sent continuously using a modulation frequency of 15 kHz. As mentioned previously, the Manchester code leads statistically to a message composed of two main pulse widths separated by front edges. In our case, the elementary modulation width is around 400 clock ticks of the microcontroller. The accuracy and the stability of the clock of the microcontroller clock are provided by a 20 MHz external quartz crystal and are good enough so that there is no need to synchronize the emitter and reception modules. The transmission of the clock is also not required and the system is thus running with asynchronous link which is easier and cheaper.

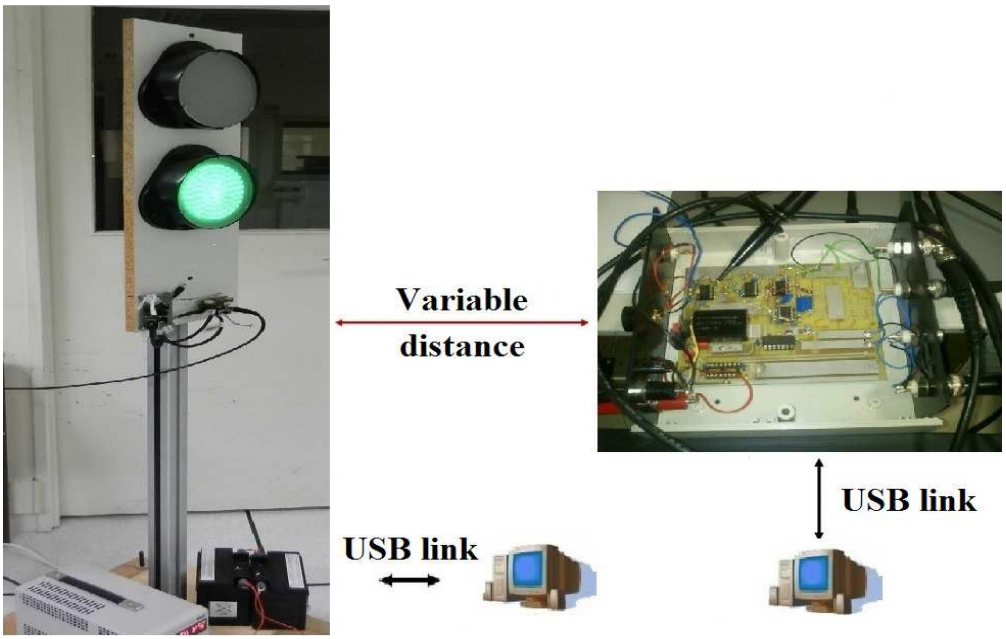

Fig. 2.10: Experimental setup for the experimental pulse width measurement

The distribution width measurements are illustrated in Fig. 2.9 for approximately 5000 bits, for each code. For Manchester case, one can see two groups of peaks: one around 400 ticks

and the second one around 800 ticks (twice the first width). The two groups are divided into two subgroups because of low-level and high-level values. This phenomenon is due to the triggering electronics part. The threshold is asymmetrical to separate low and high-level values. The low-level is indeed shorter than the high one. This asymmetry is not necessary but it is a convenient way to distinguish the two values. The amplitudes of the peaks are lower for the second group because the message sent is not random. It has been verified that the amplitude is modified when changing the message. One can see also that the four distributions are clearly separated. The most important thing is that the two groups are fully kept away from each other. The microcontroller is then counting the width of the pulses with high frequency clocks and determines the digital information easily.

The pulse length distribution for the Miller code is presented in Fig. 2.9b. This time, there are three groups of peaks: the elementary width of 800 ticks and one and a half and two times this value. Also, each of the groups is divided into two subgroups for low and high levels values. In the same manner, the amplitude is only significant of the specific sent message which is not purely random. These distributions are useful to adjust the tolerance parameters on the detection threshold for the embedded microcontroller software.

Once again, the pulses are less affected by distortion in the case of the Miller code, confirming the simulation results. However, in this case the difference between the two codes is less significant.

It can be noticed that in the case of this receiver the different width pulses are kept separated. The separation is achieved and experimentally verified for a variable distance between emitter and receiver, which can go up to 50 meters. This separation is accomplished by maintaining the SNR level as high as possible. For this purpose several hardware techniques were used. The optical part made in cooperation with Valeo industry has an important role in the SNR enhancement. It limits the receiver field of view reducing the noise and it focuses the light on the photodiode. Also, an important SNR improvement is due to the Automatic Gain Control (AGC) circuit which is continuously monitoring the signal level and adjusts the gain corresponding for the optimal value. The AGC is responsible for the control of a gain selection block and also of the adjustable bandwidth transimpedance circuit. However, in noisy conditions (emitter-receiver distance beyond 50m) the widths get wider, and the separation between different width pulses

cannot be maintained, generating decoding errors. With the SNR improvement techniques mentioned above, the VLC receiver was able to achieve a BER lower than 10^{-7} for both the codes.

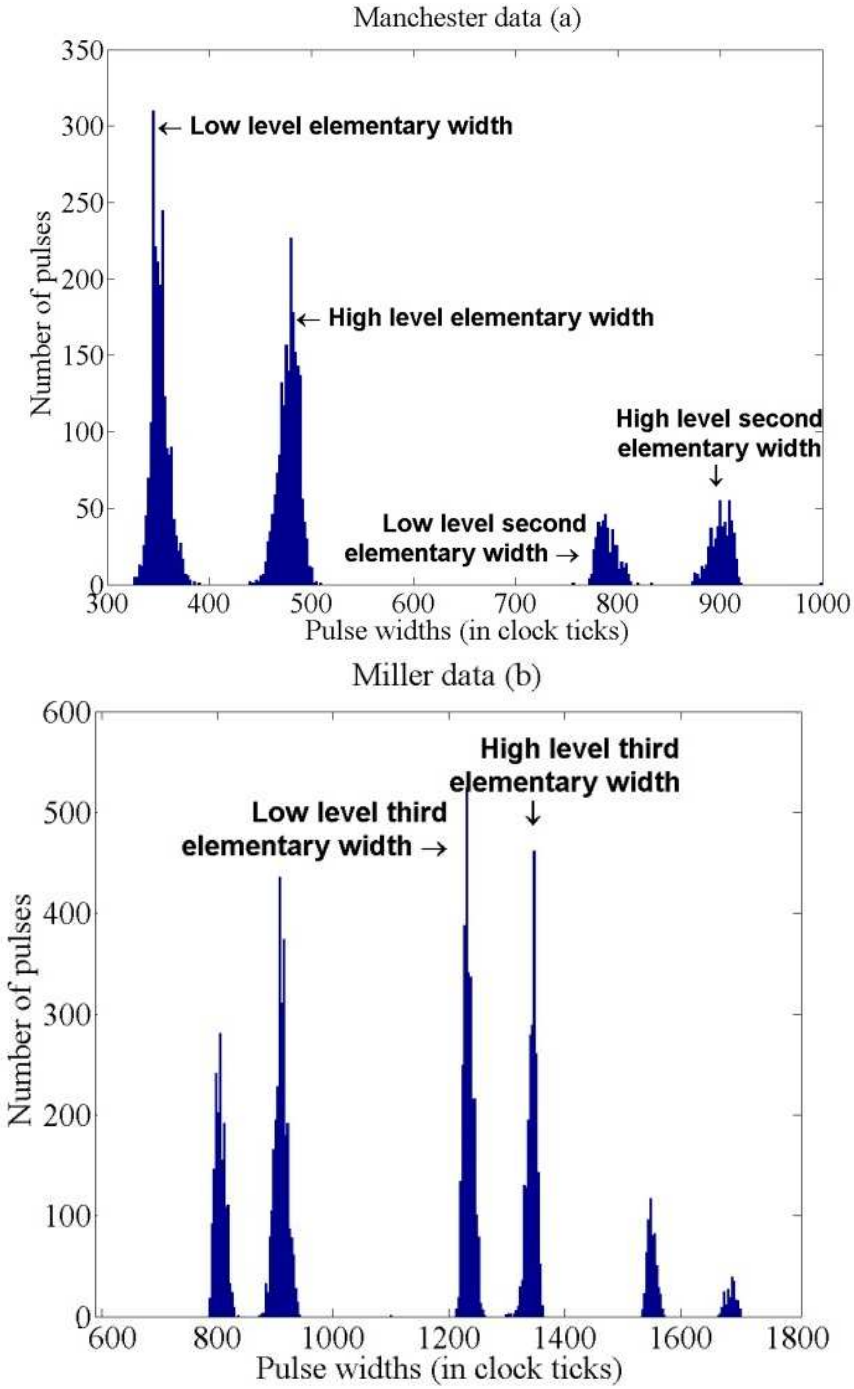

Fig. 2.11: Histograms of received pulse widths for both Manchester and Miller configurations; a) Manchester case b) Miller case

2.4 Concluding Remarks

This chapter presents a comparative analysis over the coding techniques used in VLC, focusing on the Manchester and on the Miller codes. The results show that in terms of BER, up to the 10^{-7} level, Manchester and Miller code have similar results, which was experimentally verified. However, in terms of spectral distribution Miller code clearly outperforms Manchester code, offering the premises for MIMO applications. Since the IEEE 802.15.7 standard, choses the usage of the Manchester taking into account its flickering performances, this report also analyses the flickering performances of the Miller code. The results show that even at modulation frequencies as low as 11.67 kHz, the flickering effect is very limited. However, the effects of this limited flickering must be further investigated, to determine if there is any negative effect on the human health.

Since the VLC channel can be characterized as a noisy one, this chapter presents an analysis over the noise effect on the VLC signal pulse width. It investigates both the Manchester and Miller codes providing both simulation and experimental results. The results show that as the SNR decreases, the pulse widths are more and more affected by distortion, which causes decoding errors. It can be observed that due to its nature, the Miller code signal is easier to filter, but it is affected by stricter tolerances limit, which is the main cause for errors. In the case of the Manchester code, the filtering is less effective but it catches up due to its higher tolerance to pulse width variations.

To conclude this section, one can say that the Manchester code is adequate for single channel communications whereas in the MIMO scenario, the Miller code is better suited for its channel usage superiority. Besides the multi-channel capabilities, the Miller code exhibit approximately similar performances in flickering, noise sensitivity and BER.

3. VLC Matlab/Simulink Model

3.1 Introduction

Simulations are a useful tool to reproduce the behavior of a complex system. They enable one to estimate the performances of a system and to gain insights into a technology. Generally, the simulation processes rely on the theoretical and on the numerical analysis of the behavior of the system being modeled. However, these analyzes are built on different approximations and estimations, making the precision of the results to be dependent of the accuracy of the implemented model. Even under these circumstances, the simulations are extremely useful in testing different setups and configurations, offering valuable information which helps optimizing the system and its performances. Another benefit of the simulations is the possibility of reproducing certain conditions or scenarios in a repetitive manner, and in a time-efficient way. From this point of view, the simulations represent a necessary step towards the implementation and the testing of a hardware system.

In order to perform an analysis concerning the performances of the VLC, a Matlab/Simulink model has been developed and implemented. The model integrates a basic VLC emitter, the communication channel and a VLC receiver which uses Digital Signal Processing (DSP) techniques for data recovering. The functionality of these components will be detailed in the fallowing sections.

The novelty and the unicity of the proposed model are within its structure. The model was developed with limited usage of the Matlab/Simulink built-in blocks, but with the help of coded blocks. The advantages of this approach are numerous since the simulation replicates more closely what happens inside the real hardware equipment. Also, using this approach the resemblance between the implemented model and a numerical system developed in a similar manner is very high as long as the settings of the development board are close to the ones from the simulation model (e.g. sampling frequency, ADC resolution). This way, the code can be easily fit in a microcontroller that will produce results close to the simulated ones.

The motivations and the objectives of this study are:

i) to determine if the proposed receiver architecture is well suited for VLC;

ii) to determine the noise influence on the VLC BER performances;

iii) to determine the data rate influence on the VLC BER performances;

iv) to determine the influence of message length on the VLC BER performances;

v) getting an overview of the limits for a decent communications under diverse conditions;

vi) proposing and testing a configuration for a self-adjusting VLC receiver;

vii) implementing and testing an adaptive digital filter which will be required for Multi Input Multi Output (MIMO) applications;

viii) least but not last, this simulation is a first step towards the development and the implementation of VLC receiver that uses digital signal processing as an alternative or as a complement for the classical analogical processing.

Fallowing is given the synopsis of the VLC architecture (model), with a brief description of the signal processing blocks that have been used. The end of this chapter presents the simulation results and several conclusions that come out of these results.

3.2 Simulation premises

The simulation uses the premises of a direct LoS between emitter and receiver, necessary for a VLC system to work. Surrounding surfaces can cause unwanted reflections or can scatter the VLC signal, creating multipath effects that can affect the communication. However, it has been demonstrated that the multipath effects do not affect VLC [16], except in the case of short distances, which are not usually fulfilled under normal traffic conditions. For this reason, non-LoS and multipath signal are not included in this simulation.

In the simulation, the clock of the receiver is not synchronized with phase locked-loop for simplicity. The usage of asynchronous transmission is encountered in hardware systems in order to maintain the complexity level and the implementation cost as low as possible [19]. However, the frequencies involved (few kilohertz) are low enough and the decoding system has no need of time accuracy.

Numerous sources [1] suggest that in wireless communications the message length has an influence on the BER performances. This problem is extremely stringent for the RF based communications, where the message length influences the communication performances due to the mutual interferences of the different nodes [1]. Concerning the VLC, an elaborated study concerning the influence of the message length on the BER performances is not available. In

order to determine this influence on the VLC, three message lengths were investigated in different SNR conditions and at different data rates. It was considered a short message of 120 bits, a medium size message of 600 bits and a long message of 1024 bits. Regarding the normal message length for communication-based vehicle safety applications, [16] based on the requirements from [31] considers the message length of 481 bits to be representative. A close message length is considered in [1], where 500 bits were used. Based on these considerations, the 600 bits message length can be considered appropriate for VLC, whereas 120 and 1024 bits are used as references in order to determine the behavior of the communications. In traffic safety communications, the message length and the required information fields vary depending on the application. The USA Department of Transportation (DOT) has defined the minimum information field requirements for different situations. In the case of a traffic light, the minimum information requirements are presented in Table 3.1.

Table 3.1 Traffic Signal Violation Warning Data Message Set Requirements [31]

Description	Number of bits
Traffic signal status information	
Current phase	8
Date and time of current phase	56
Next phase	8
Time remaining until next phase	24
Road shape information	
Data per node	32
Data per link to node	72
Road condition/surface	8
Intersection information	
Data per link	120
Location (lat/long/elevation)	96
Stopping Location (offset)	32
Directionality	16
Traffic signal identification	48
Message type	8
Total	528

As previously mentioned, the IEEE 802.15.7 standard specifies for outdoor low data rate applications the usage of OOK with Manchester coding. The data rates mentioned in this case are 11.67, 24.44, 48.89, 73.3 and 100 kb/s. In this chapter, the performances of these five communication frequencies will be further investigated, in order to determine their influence on the communication performances. The effect of noise on each of the data rates will also be subject to simulations.

3.3 The VLC channel characterization

The VLC performances are strongly influenced by the communication channel. A VLC channel can be modeled as a baseband linear system, with instantaneous power *X(t)*, output photocurrent *Y(t)* and impulse response *h(t)*. The channel is subject to signal independent additive noise as presented in Fig. 3.1 and expressed in eq. 3.1.

$$Y(t) = RX(t) \otimes h(t) + N_{Total}(t) \tag{3.1}$$

where *R* is the detector responsively (A/W), and ⊗ indicates the convolution.

Since *X(t)* is the optical instantaneous power, the channel input is always positive, so *X(t)*>=0. Another important aspect that need to be pointed out is the linear relationship between *X(t)* and *Y(t)*.

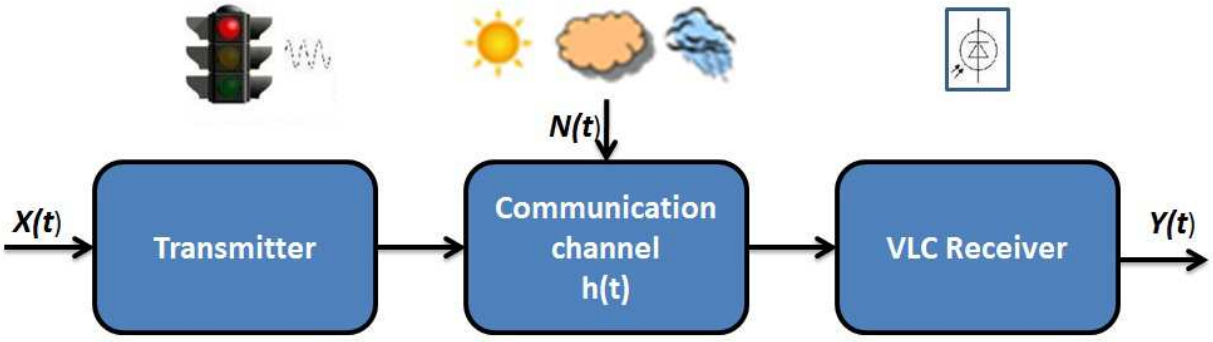

Fig. 3.1: Communication model

3.3.1 Noise effect on the VLC channel

Outdoor VLC applications are subject to multiple external noise sources which affect the communication. For VLC, the major noise source is represented by the background light. The background light can be either from artificial sources either from natural sources. The bright sky light and the direct sun light are the natural light sources. These two sources are the most perturbing for a VLC system due to their high power, which in some of the cases can saturate the photoelement, making it blind. The artificial noise sources are represented by classical light sources with no communication capabilities such as incandescent sources or neon lights which produce a strong parasitic 100 Hz signal. However, there are studies that show the negative influence of the artificial lighting sources up till frequencies of tens of kilohertz [32]. In most of the cases, these sources have a much higher power compared with the power of the desired signal. Besides these unmodulated light sources, data transmitting light emitters can also affect the VLC.

Both sunlight and artificial light affect the communication by introducing a high intensity shot noise component. The shot noise is proportional to the optical noise power incident on the receiver. The effect of the shot noise can be minimized by using optical filters, but still this is a perturbing noise source limiting the communication's performances. In day-time outdoor communications shot noise is the dominant noise component. The shot noise intensity is proportional to the photodetector area and is given by eq. 3.2:

$$N_{shot} = 2qIB \tag{3.2}$$

where q is the electronic charge ($1.602 \cdot 10^{-19}$ coulombs), B is the detector bandwidth and I is the produced photocurrent and given by eq. 3.3:

$$I = RP_{total} \tag{3.3}$$

According with eq. 3.3, the shot noise induced in the receiving circuit is influenced by the total optical power incident on the effective light collection area, which is given by eq. 3.4.

$$P_{total} = P_{noise} + P_{signal} \tag{3.4}$$

The formula above includes the shot noise contribution of both useful signal and of the noise signal. It can be observed that the shot noise is proportional with the total detected optical

power incident on the photoelement. However the contribution of the useful signal to the shot noise is quite limited compared with the one of the background noise or even with the one of the preamplifier thermal noise. From this consideration, the shot noise can be considered as a signal independent noise. Due to the high intensity, the shot noise component can be modeled as white Gaussian noise.

The preamplifier thermal noise is also a perturbing factor for the VLC receiver. In the absence of background light, the preamplifier thermal noise is the predominant noise source. This noise type is also a signal independent Gaussian noise. The value of the preamplifier thermal noise is given by eq. 3.5.

$$N_{thermal} = \frac{4KTBN_{circuit}}{R} \tag{3.5}$$

where K is Boltzmann's constant ($1.381 \cdot 10^{-23}$) and T is the temperature.

Under these conditions, the total noise is given by:

$$N_{total} = \sqrt{{N_{shot}}^2 + {N_{thermal}}^2} \tag{3.6}$$

Since both the shot noise and the thermal noise are signal-independent and Gaussian, one can conclude that the total noise of the VLC channel can be modeled as signal-independent Gaussian noise.

3.3.2 Channel DC gain in Line of Sight (LoS) conditions

A VLC emitter is considered a Lambertian emitter and its radiant intensity distribution (W/cm^2) can be modeled according with eq. 3.7.

$$R_0(\varphi) = \left(\frac{m+1}{2\pi}\right) cos^m \varphi \tag{3.7}$$

The order m is depending on the half power angle (HPA) of the emitter in accordance with eq. 3.8.

$$m = -\frac{\ln 2}{\ln\left(cos\phi_{1/2}\right)} \tag{3.8}$$

where $\phi_{1/2}$ is the transmitter semi angle;

In this case the irradiation pattern of the VLC emitter is given by eq. 3.9.

$$R_E = P_t R_0(\varphi) \tag{3.9}$$

Since the light intensity is decreasing with the square of the distance, the irradiance at a receiver situated at distance *d* is and an angle φ, according with the transmitter, given by:

$$I_s(d, \varphi) = \frac{P_t R_0(\varphi)}{d^2} \tag{3.10}$$

In this case, the received power at the receiver side (P_r) is depending on the effective signal collection area (A_{eff}) of the receiver.

$$P_r = I_s(d, \varphi) A_{eff}(\psi) \tag{3.11}$$

where A_{eff} is given by:

$$A_{eff}(\alpha) = \begin{cases} A\cos\psi, & \psi < FOV \\ 0, & \psi > FOV \end{cases}, \qquad FOV < \pi/2 \tag{3.12}$$

ψ angle of incidence on the receiver;

The value of A_{eff} can be increased with the usage of an optical concentrator that ads a gain to this value.

In the absence of an optical concentrator, the channel dc is given by:

$$H(0)_{LOS} = \begin{cases} \frac{(m+1)}{2\pi d^2} \cos^m \varphi \, \mathrm{A} \cos(\psi), & 0 < \psi < FOV \\ 0, & \psi > FOV \end{cases} \tag{3.13}$$

It can be observed that by reducing the angle of emission, and therefor *m*, increases the directivity of the radiation pattern which significantly increases the communication range.

The optical power received by the receiver is:

$$P_r = H(0)_{LOS} P_t \tag{3.14}$$

Under these conditions, considering *R* the detector conversion efficiency, *B* the bandwidth and N_0 the noise power spectral density, according to [33] the electrical SNR is given by:

$$SNR = \frac{\sqrt{2} R P_r}{\sqrt{B N_0}} \tag{3.15}$$

3.4 The VLC emitter model

The synopsis of the VLC emitter model is represented in Fig. 3.2. The functions involved are user centered and easy to use. Based on the data rate and on the coding settings, this block transforms the text data message into an OOK modulated message that is ready to send through the communication channel. This block performs the ASCII to binary conversation, the message coding (Manchester, Miller, 4B6B) and the message packaging according with the data frame format which will be presented in Section 3.4.1. The frame will be further modulated according to the selected data rate by a Matlab/Simulink *Repeating Sequence Stair* block. For test purposes the message length is limited to 128 characters or 1024 bits, but if required the message length can be increased.

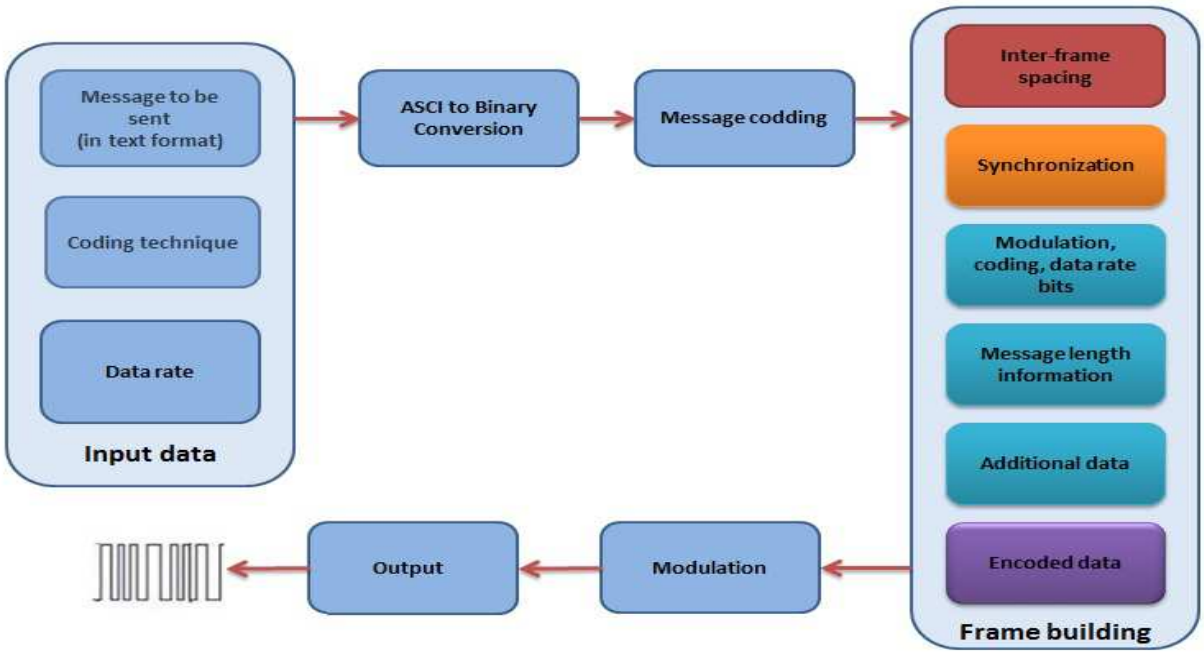

Fig. 3.2: Synopsys of the VLC receiver

The structure of the proposed model is similar with the one of a real VLC emitter. In this case the microcontroller builds the data frame according with the user's preferences and the frame structure, whereas with the help of a digital power switch the LEDs are controlled. The output signal of the emitter model is shown in Fig. 3 i).

3.4.1 Considerations on the frame structure

The structure of the frame is based on the structure from the IEEE 802.15.7 standard but it has been simplified and adjusted. As presented in Fig. 3.3 the structure of the frame contains a header field and a data field. The header field consists of 43 bits. It begins with a 17 bits preamble used for synchronization. This field enables the receiver to achieve synchronization. It consists of a sequence of zeroes and ones and it can have a variable length. Compared with the preamble from the upper mentioned standard which contains a variable size preamble of at least 64 bits, the header contained by the implemented frame is significantly shorter. The length of the synchronization is a trade-off between frame overhead and false data acquisitions.

The fallowing field of the header is the Modulation and Codding Scheme (MCS) field. The MCS field uses 6 bits to provide the receiver with information regarding the selected modulation, coding technique and also about the data rate.

The next field of the header, consisting of 10 bits, is the Message Length (ML) field, which provides the receiver with information concerning the number of bits to be received.

The next header field consists of 8 bits that for the moment are not used. These bits can be used to provide information about dimming or other type of data that could improve the data decoding process.

The header field is transmitted at the lowest frequency, namely 11.67 kHz using OOK modulation. From the header, for the preamble filed there is no use of any line codding, whereas for the other three fields Manchester code is used for data encoding.

The data field has a variable length which can extend from 8 to 1024 bits. This field is transmitted at variable frequency, between 11.67 kHz and 100 kHz according with the data rates specified by the IEEE 802.15.7 standard for outdoor low data rates applications. According with the same standard, the data bits and the header bits are transmitted using the Manchester codding.

Fig. 3.3: Structure of the data frame

Since the purpose of this study is to investigate the effect of noise on the quality of the data transmission and on the BER at the physical layer, the use of error correcting codes has been put aside. However, checksum fields can be easily added for both header and data fields.

3.5 The VLC receiver model

The proposed model aims to be a close replication of a real VLC receiver. It uses the same functionalities and the same working principle. At the same time, it tries to address the challenges imposed in real situations. Basically, the system is meant to be a self-adjusting one, able to respond and to adapt to the environment and to different working conditions (such as mobile conditions or different data rates).

The proposed model addresses several key challenges regarding its adaptability. The receiver model is designed in order to be able to receive and properly decode messages coming at different data rates. This requires an adaptive filtering mechanism able to distinguish between several frequency bands, and also able to commute between different frequency bands. This way, the incoming signal containing the data is situated in the filter's band-pass at all time.

Dynamic conditions as the ones encountered in traffic situations, where the vehicles are in continuous movement lead to significant variations of the emitter-receiver distance. This phenomenon involves significant variations of the SNR. This problem can be addressed by using an Automatic Gain Control (AGC) mechanism, which maintains a constant signal level, preventing photodetector saturation at short distances whereas insufficient signal amplification is prevented at long distances.

The proposed receiver model was developed with limited usage of Matlab/Simulink blocks but uses instead Simulink user-defined functions, Matlab Function block. The MATLAB Function block allows flexible programming, using Matlab code, which can be used in a Simulink model. This capability is useful for coding algorithms that are better stated in the textual language of the MATLAB software than in the graphical language of the Simulink product. Another advantage of this approach is that it gives an inside view over the signal processing. Even if this approach is a time consuming one, because it requires that almost every aspect of the simulation to be built from zero, it has the advantage that is a step ahead when implementing the model on a hardware DSP system, since the Matlab code is very similar with the C code. The synopsis of the VLC receiver is presented in Fig. 3.

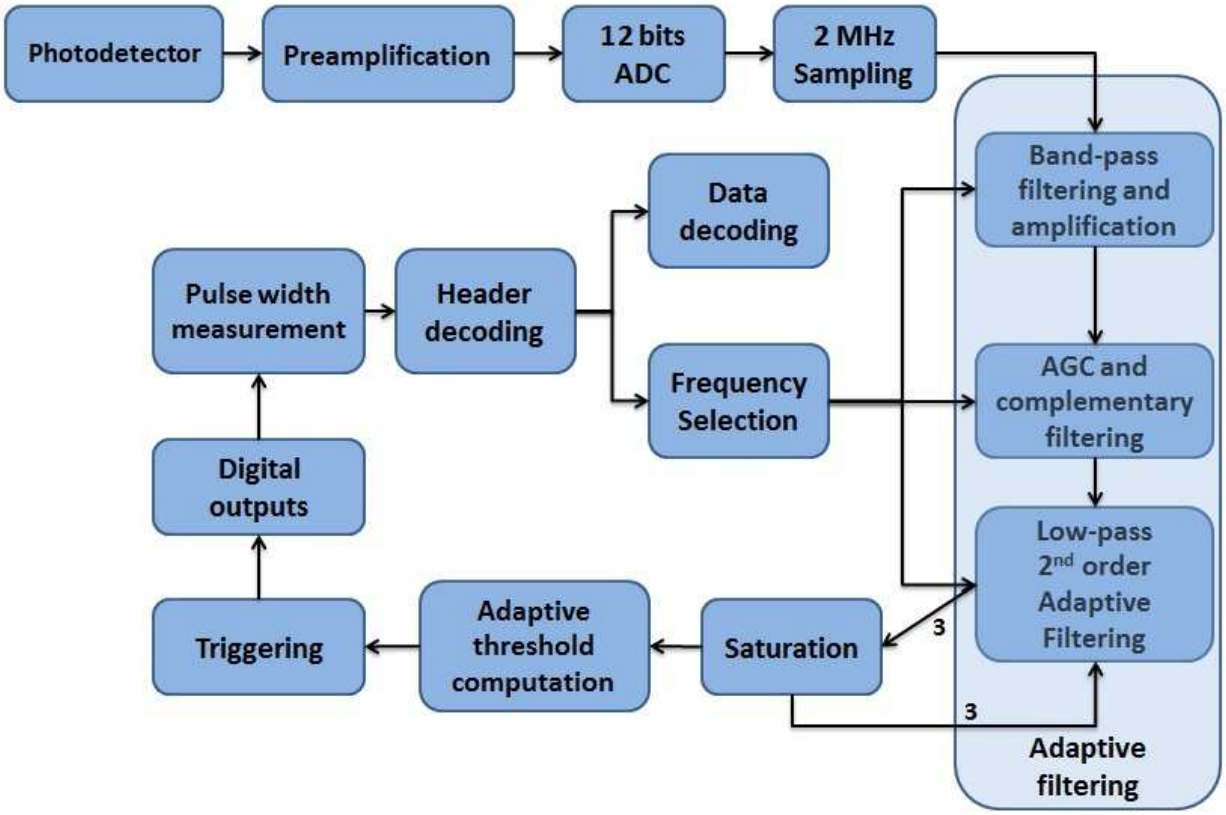

Fig. 3.4: Synopsis of the VLC receiver model

3.5.1 VLC Receiver System Model Blocks

Following is a brief description of the blocks used in the receiver model. The parameters and the working principle of the blocks are provided.

3.5.1.1 Fixed gain

The Gain block multiplies the input by a constant value (gain). Since the degradation of the signal is proportional with the square of the distance, this block is required as a pre-amplification block. Complementary amplification is required, depending on the strength of the received signal.

3.5.1.2 ADC Quantizer Block

The block is set to sample the signal at a specified rate of 2 MHz and with a resolution of 0.008 V corresponding to a 12 bits ADC resolution for a 3.3 V input. This block provides the fallowing block with numerical values that will be used for the digital signal processing.

3.5.1.3 Automatic Gain Control

This block helps maintaining a constant signal level required for proper message decoding. It adds a complementary gain to the fixed gain. The complementary gain value is computed based on the current value of the signal. To determine the current signal amplitude in an accurate way, a number of readings are performed and based on these reading an average value is considered as the signal amplitude value. The value of the gain is updated only if required with a certain frequency. The AGC block ensures a high and steady amplitude level. It uses an optimal signal value and minimum and maximum thresholds. Whenever the signal's amplitude rises above or it gets bellow the maximum or the minimum thresholds, the new gain value is computed in order to set the signal at the optimum value. This process is illustrated in Fig. 3.5.

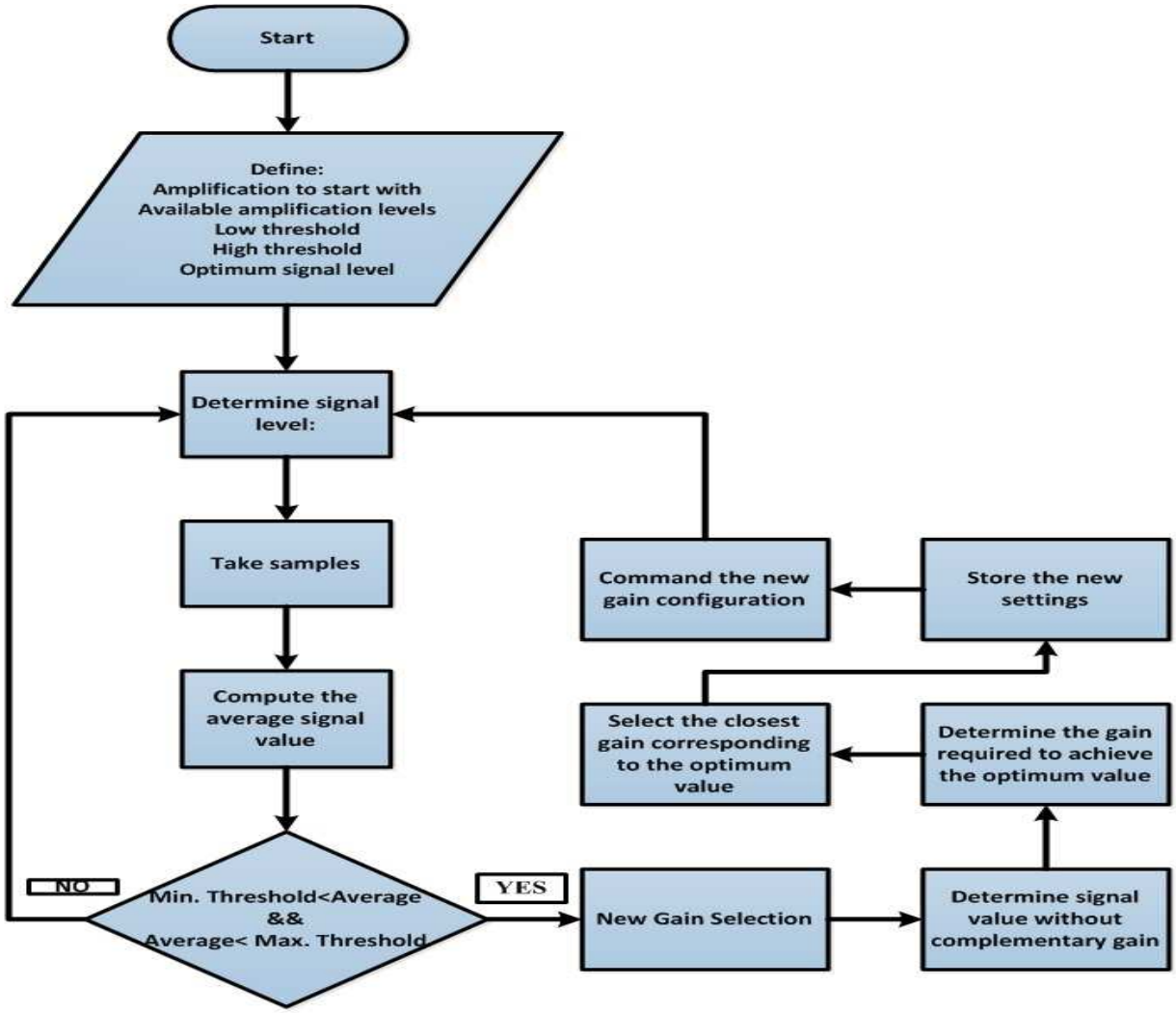

Fig. 3.5: Automatic Gain Control flowchart

3.5.1.4 High-pass Butterworth Filter

The classical lighting sources without data communication capabilities produce low frequency noise components. For example, the neon lights produce a strong 100 Hz parasitic signal which is adding to the useful signal. The high-pass 2^{nd} order Butterworth filter block removes these low frequency noise components. The cut-off frequency of the filter is set at 1 kHz.

3.5.1.5 Adjustable Butterworth Low-Pass Filters

The adjustable low-pass filters remove the unwanted high frequency noise component of the signal. These are two inputs filters: one input is for the input samples (signal to filter) and the second input is for the cut-off frequency. The second input is connected with the message decoding block, which is continuously commanding the cut-off frequency. As detailed in the previous section, the data frame consists of a constant frequency header and of a variable frequency part containing the data. While the message decoding block is waiting for an incoming signal it commands the filter so that the base 11.67 kHz frequency of the header to be in the band pass. After synchronization and header receiving the message decoding block decodes the header containing the data rate frequency and command the filters according with the new frequency. The impact of a Butterworth 2^{nd} order filter on a noisy input signal is shown in Fig. 3 iii).

3.5.1.6 Saturation Block

This block removes part of the high frequency noise and helps improve the signal. Basically, these block cut a 10% part of the signal, which leads to a significant improvement of the signal quality.

3.5.1.7 Partial Pulse Reconstruction Blocks

Several reconstructing stages are used to gradually remove the effects caused by noise interferences. These blocks are used for a partial and progressive reconstruction of the signal. The output of such a block is a partial square signal which represents an intermediate step towards the signal reconstruction. Fig. 3 iv) shows the output of a partial pulse reconstruction block.

3.5.1.8 Pulse Reconstruction Blocks

This block is responsible for the final signal reconstruction. It outputs the replication of the transmitted square signal. The triggering is performed based on an adaptive threshold algorithm, meaning that the threshold is computed individually for every pulse, based on the previous pulses. The adaptive threshold mechanism allows improved signal reconstructions. The input and the output signal of the pulse reconstruction block are shown in Fig. 3 v) and vi).

3.5.1.9 Pulse Width Measurement Block

Since the decoding is performed based on the detection of the rising and falling edges and on the pulse width measurement, a block responsible for these operations is strongly required. This block identifies the beginning and the end of each pulse and determines its width. This information is transmitted to the Data Decoding block.

3.5.1.10 Data Decoding and Processing Block

This block is responsible for the final processing of the signal. It is responsible for synchronization, header decoding and message decoding. As mentioned previously it is also responsible for the command of the filter frequency selecting.

Another operation performed by this block is the data post processing. The decoding is made in real time. It provides information regarding the quality of the communications such as the total number of bits, the number of error bits, the total number of messages and the number of messages containing decoding errors.

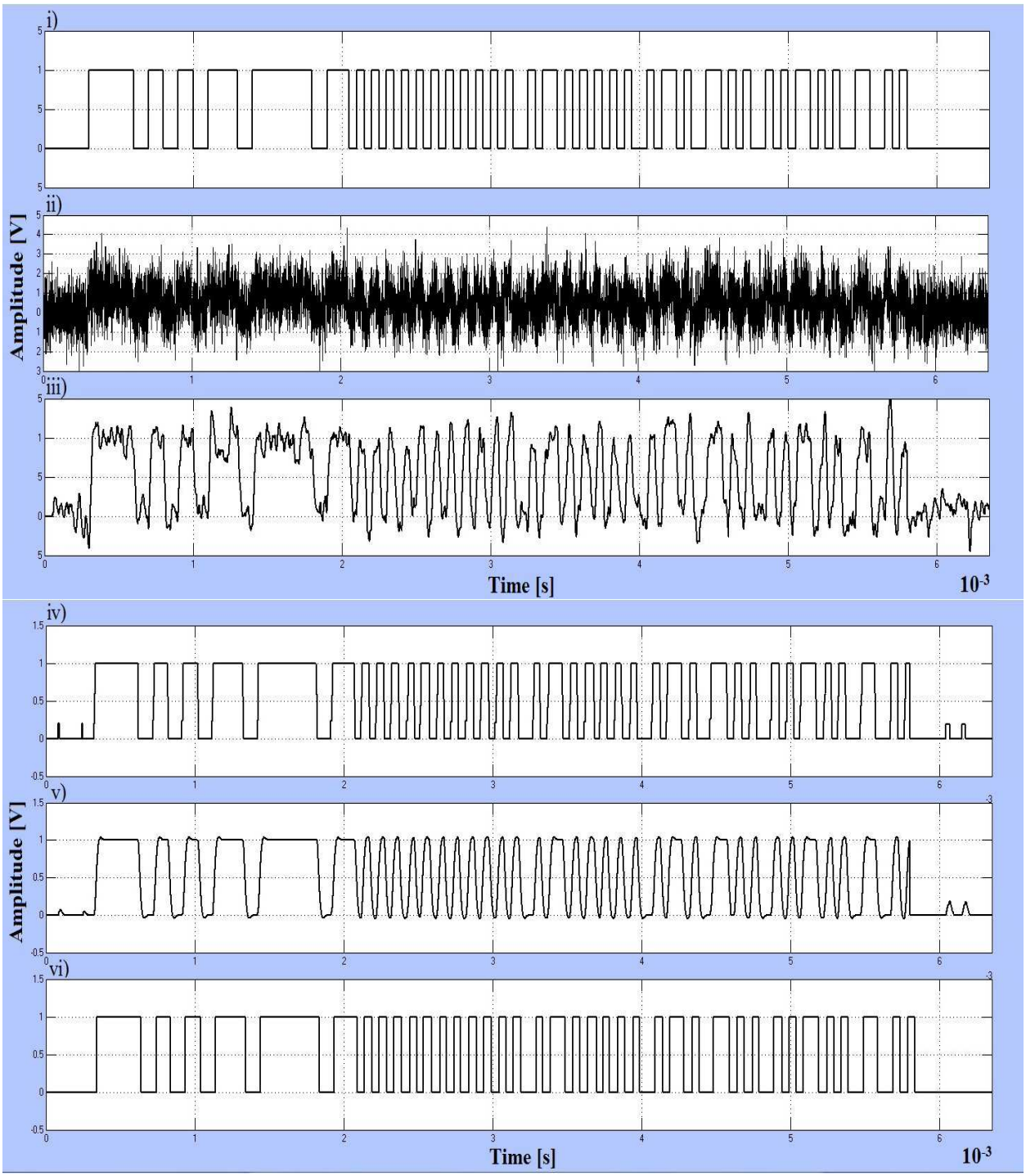

Fig. 3.6: Modifications of the signal throughout the blocks of the model: i) representation of the original Manchester encoded message, ii) representation of data message with AWGN (SNR=1 dB), iii) output of a 2nd order Butterworth filter, iv) representation of the signal after the first reconstruction attempt, v) input for the signal reconstruction block, vi) representation of the reconstructed square signal used for data decoding.

3.6 The Performance Results of the VLC Model

This section presents the BER performances for the five communication channels defined in the IEEE 802.15.7 standard, in the presence of different SNR levels for an optimized DSP system described in the previous section.

The results show the effect of the noise on the BER performances. It can be seen that as the SNR decreases the BER increases, which is a normal and an expected result. It can be observed that the BER increase is not as strong in the case of the lower frequencies. The simulation results clearly show that higher frequencies are more sensitive to noise. One of the main reasons for this is the insufficient filtering which makes the signal reconstruction more difficult. The manner in which the noise affects the signal reconstruction and the pulse distortion it induces were described in detail in Section 2.3.3. As it can be seen, the data rate has a major influence on the BER performances.

The results show that for higher data rates, higher levels of SNR are required. Since the signal strength is decreasing as the range is increasing the higher data rates are recommended for shorter range whereas as the distance is increasing the data rate should be decreased.

The results also show how the message length influences the BER performances. It can be noticed that this factor does not influence significantly the communication performances. So, for normal priority messages any message length between 120 and 1024 bits could be used, but, as mentioned in the previous section, the average length of a safety related message is around 500-600 bits. This test is just a guidance test since depending on the application different message lengths are specified and the use of predefined lengths is not efficient.

The results can be used in order to set up the requirements for different configurations. For example, traffic safety applications would require a BER above 10^{-6}. The results can be used in order to adapt the data rate to the noise conditions.

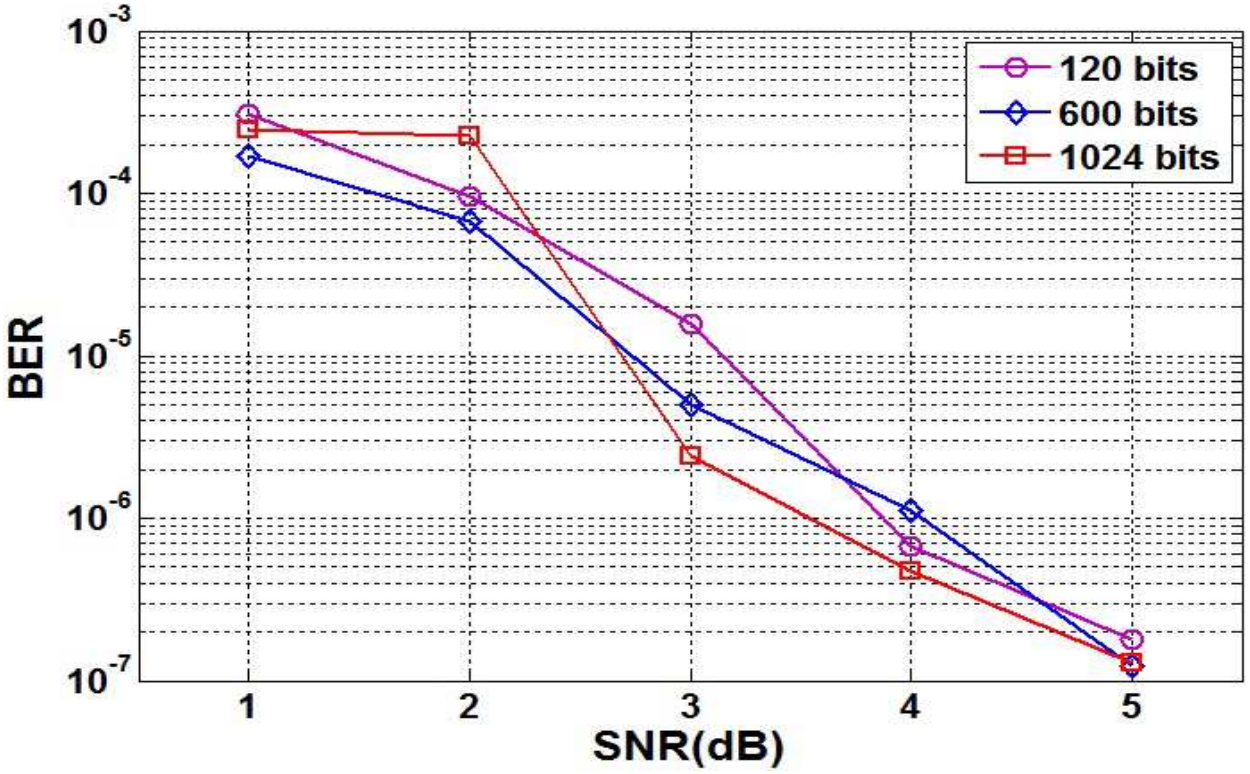

Fig. 3.6: BER performances at 11.67 kHz

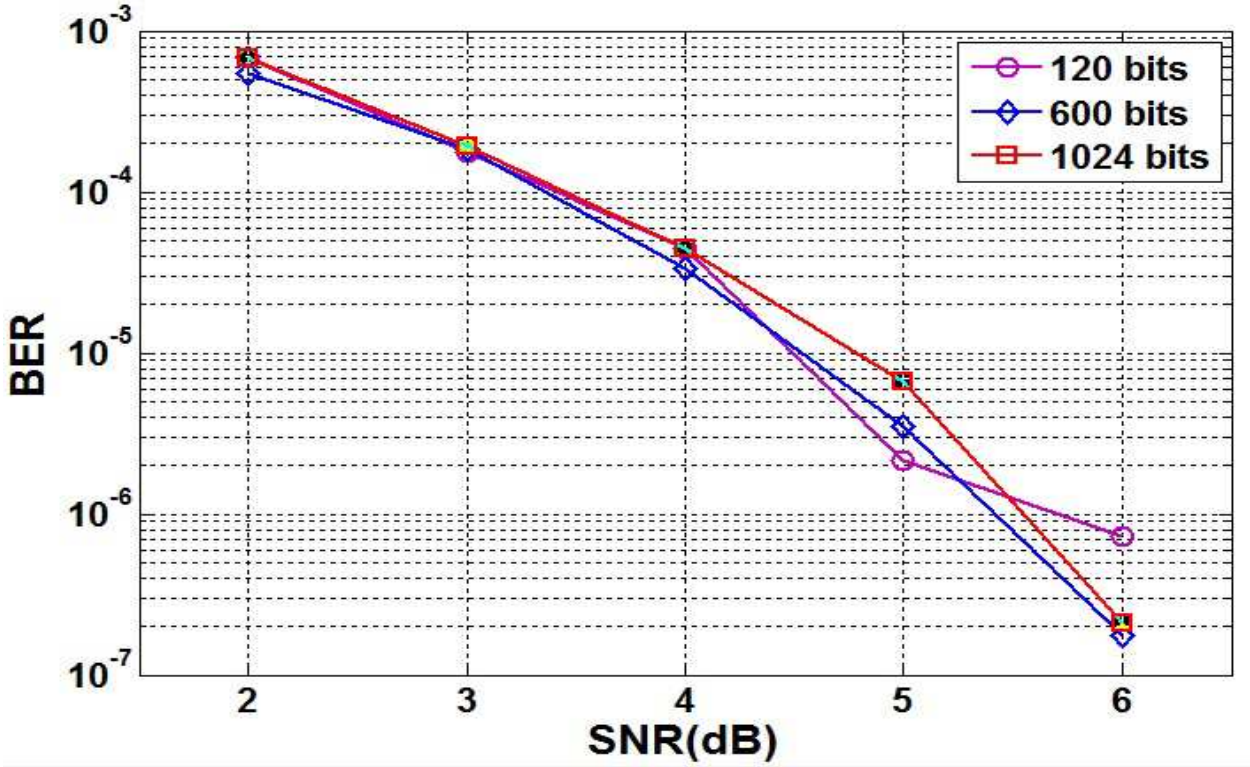

Fig. 3.7: BER performances for 24.48 kHz

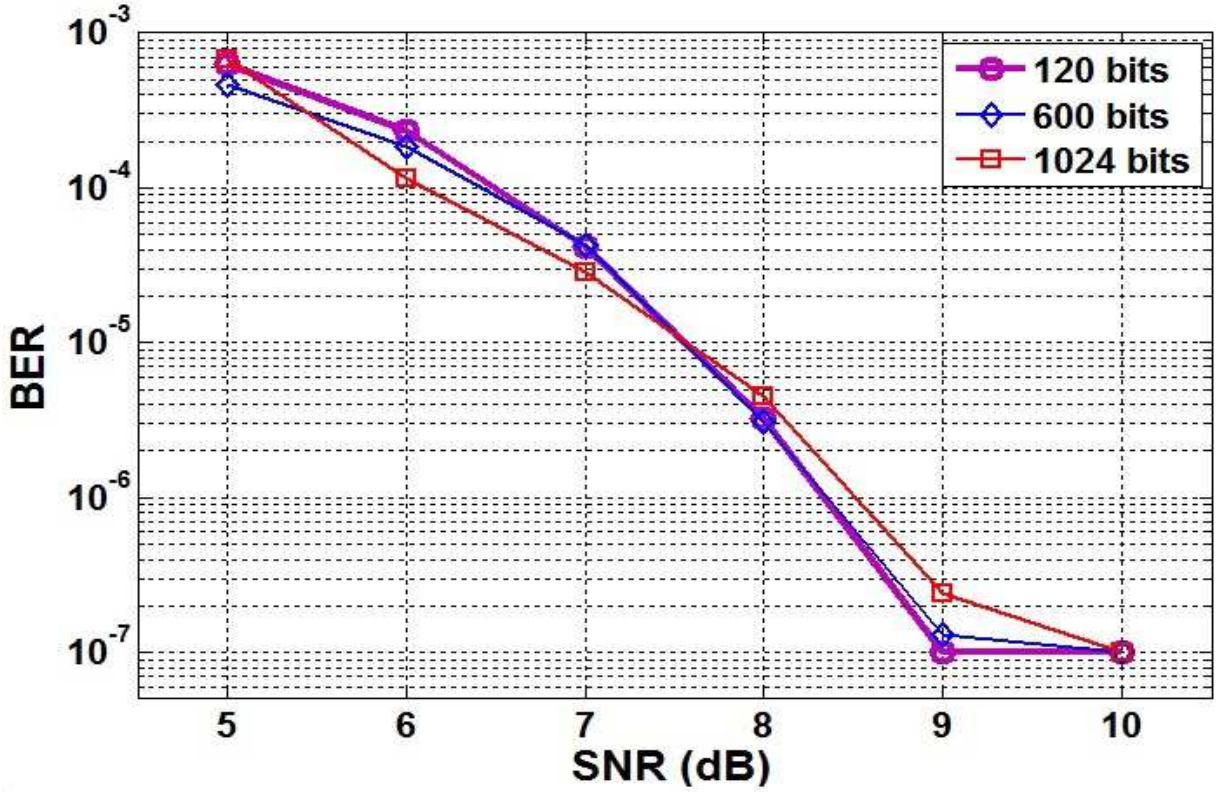

Fig. 3.8: BER performances for 48.89 kHz

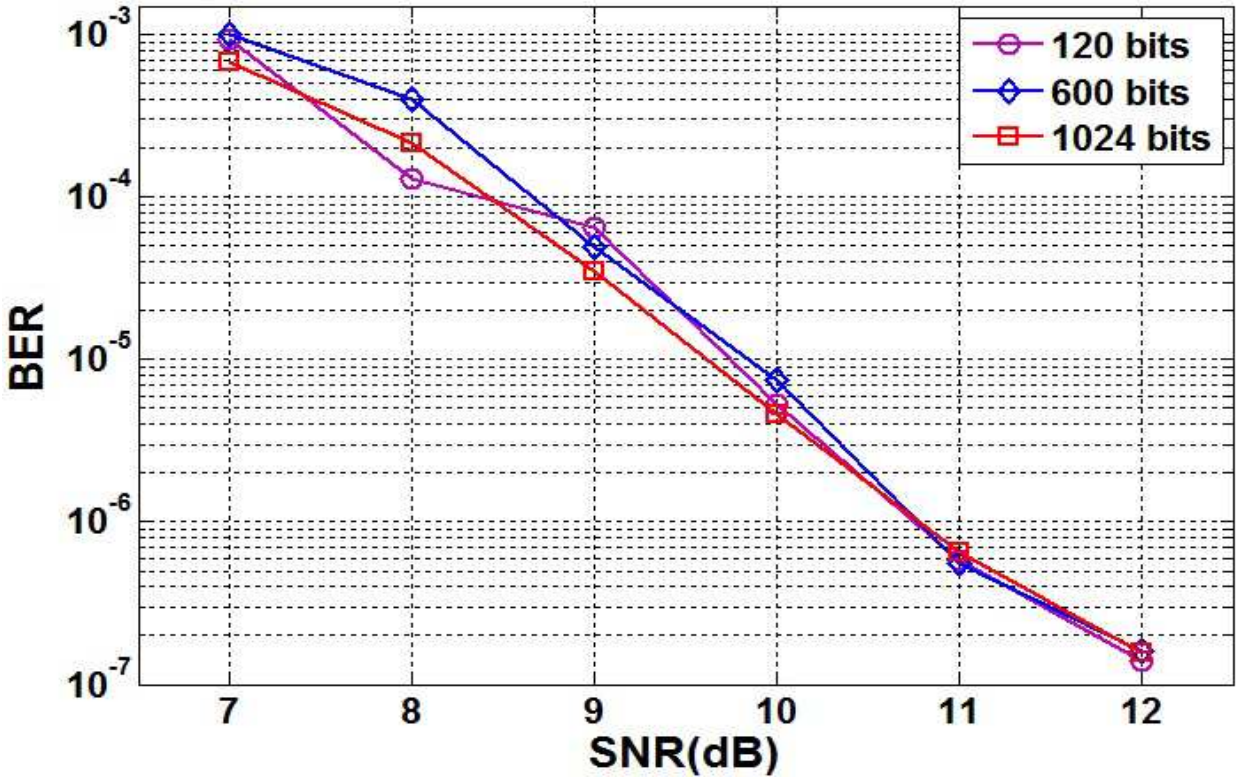

Fig. 3.9: BER performances for 73.30 kHz

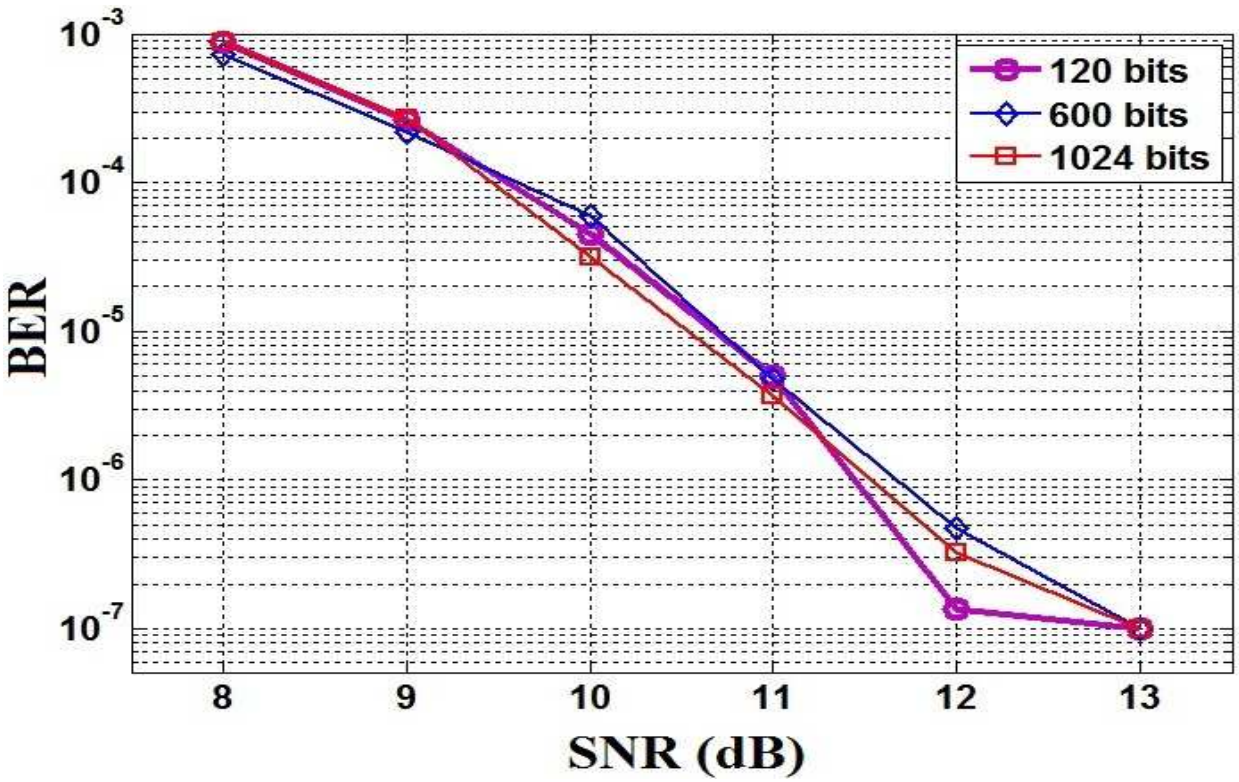

Fig. 3.10: BER performances for 100.00 kHz

The performances of the proposed model are increased due to several mechanisms. The AGC block ensures a high and steady amplitude level, enabling the decoding for various input signals. The adaptive filtering allows the signal to receive messages at different frequencies without adjusting the signal. The filtering is made in several stages, each stage removing parts of the signal. The filtering performances are influenced by several factors: the order of the filter, the quality of the ADC conversion, the sampling frequency and namely the number of samples for each bit. An increased number of samples allows for better filtering which improves the BER. The progressive filtering along with the progressive message reconstruction that uses the adaptive threshold mechanism improves the quality of signal reconstructions and implicitly the communication performances.

3.7 Concluding Remarks

This chapter has presented an analysis over the factors that influence the BER performances of a VLC system. The analyses were performed based on simulations using VLC model implemented in Matlab/Simulink. The model was implemented mostly using user-defined Simulink functions instead of the common blocks in order to offer a higher similarity with a DSP hardware system implemented on a high performance microcontroller or on a FPGA.

Based upon the simulation results, it was observed the manner in which the noise, the data rate and the message length influence the VLC BER performances. The results are relevant for a digital signal processing system. Hardware implementation and validation of these results will be presented in the next chapter.

References

[1] S. Eichler, “Performance Evaluation of the IEEE 802.11p WAVE Communication Standard”, In IEEE Vehicular Technology Conference, 2007.

[2] K. Bilstrup, E. Uhlemann, E. Strm, and U. Bilstrup, “On the ability of the 802.11p MAC method and STDMA to support real-time vehicle-to-vehicle communication,” vol. 2009, no. 1, p. 902414, Jan.2009.

[3] World Helth Organization. (June 2011). Fact Sheet 193 – Electromagnetic fields and public health: mobile phones.

[4] Shuailong Zhang; Watson, S.; McKendry, J.J.D.; Massoubre, D.; Cogman, A.; Erdan Gu; Henderson, R.K.; Kelly, A.E.; Dawson, M.D., "1.5 Gbit/s Multi-Channel Visible Light Communications Using CMOS-Controlled GaN-Based LEDs," *Lightwave Technology, Journal of* , vol.31, no.8, pp.1211,1216, April15, 2013.

[5] N. Kumar, N. Lourenço, D. Terra, L.N. Alves, R.L. Aguiar, “Visible Light Communications in Intelligent Transportation Systems“, *IEEE Intelligent Vehicules Symposium 2012*, 748-753.

[6] M. Akanegawa, Y. Tanaka and M. Nakagawa, “Basic Study on Traffic Information System Using LED Traffic Lights*”, IEEE Transactions on Intelligent Transportation Systems*, vol. 2, no. 4, 197-203, 2001.

[7] A. Cailean, B. Cagneau, L. Chassagne, S. Topsu, Y. Alayli, J.-M. Blosseville “Visible light communications: application to cooperation between vehicles and road infrastructures“, *IEEE Intelligent Vehicles International Symposium*, 2012, pp. 1055 – 1059.

[8] Takai, I.; Ito, S.; Yasutomi, K.; Kagawa, K.; Andoh, M.; Kawahito, S., "LED and CMOS Image Sensor Based Optical Wireless Communication System for Automotive Applications," *Photonics Journal, IEEE*, vol.5, no.5, pp.6801418, Oct. 2013 doi: 10.1109/JPHOT.2013.2277881.

[9] U.S. Department of Transportation Research and Innovative Technology Administration, Report: Frequency of Target Crashes for IntelliDrive Safety Systems, October 2010.

[10] Pang, G.K.H., Liu, H., Chan, C.H., Kwan, T., “Vehicle Location and Navigation Systems based on LEDs”, Proceedings of fifth World Congress on Intelligent Transport Systems, Paper 3036, Seoul, Korea, 12-16 Oct. 1998.

[11] Pang, G.K.H., Chan, C.H., Liu, H., Kwan, T., “Dual use of LEDs : Signaling and communications in ITS”, Proceedings of fifth World Congress on Intelligent Transport Systems, Paper 3035, Seoul, Korea, 12-16 Oct.1998.

[12] Kasashima, Tatsuya; Yamazato, Takaya; Okada, Hiraku; Fujii, Toshiaki; Yendo, Tomohiro; Arai, Shintaro, "Interpixel interference cancellation method for road-to-vehicle visible light communication," *Wireless Vehicular Communications (WiVeC), 2013 IEEE 5th International Symposium on* , vol., no., pp.1,5, 2-3 June 2013.

[13] N. Kumar, D. Terra, N. Lourenço, L.N . Alves, R.L. Aguiar, “Visible light communication for intelligent transportation in road safety applications”, Wireless Communications and mobile computing conference (IWCMC), 2011 7th international, pp. 1513-1518, doi: 10.1109/IWCMC.2011.5982762, 2011.

[14] Takai, I.; Ito, S.; Yasutomi, K.; Kagawa, K.; Andoh, M.; Kawahito, S., "LED and CMOS Image Sensor Based Optical Wireless Communication System for Automotive Applications," *Photonics Journal, IEEE*, vol.5, no.5, pp.6801418, Oct. 2013.

[15] S. Yousefi, E. Altman, R. El-Azouzi, and M. Fathy, "Analytical Model for Connectivity in Vehicular Ad Hoc Networks", IEEE Transactions on Vehicular Technology, vol. 57, pp. 3341-3356, 2008.

[16] C. Liu, B. Sadeghi, E. W. Knightly, “Enabling vehicular visible light communications (V2LC) networks”, Vanet’11, Las Vegas, USA, 2011.

[17] A. Cailean, B. Cagneau, L. Chassagne, S. Topsu, Y. Alayli, M. Dimian, “Visible Light Communications Cooperative Architecture for the Intelligent Transportation System”, *20th IEEE Symposium on Communications and vehicular Technology*, Namur - Belgium, 2013.

[18] IEEE Standard for Local and Metropolitan Area Networks--Part 15.7: Short-Range Wireless Optical Communication Using Visible Light, IEEE Standard, 2011, 1-309.

[19] Cailean, A.-M.; Cagneau, B.; Chassagne, L.; Topsu, S.; Alayli, Y.; Dimian, M., "Design and implementation of a visible light communications system for vehicle applications," *Telecommunications Forum (TELFOR), 2013 21st* , vol., no., pp.349,352, 26-28 Nov. 2013 doi: 10.1109/TELFOR.2013.6716241.

[20] Elgala, H.; Mesleh, R.; Haas, H.; Pricope, B., "OFDM Visible Light Wireless Communication Based on White LEDs," *Vehicular Technology Conference, 2007. VTC2007-Spring. IEEE 65th* , vol., no., pp.2185,2189, 22-25 April 2007.

[21] Vucic, J.; Kottke, C.; Nerreter, S.; Langer, K.-D.; Walewski, J.W., "513 Mbit/s Visible Light Communications Link Based on DMT-Modulation of a White LED," *Lightwave Technology, Journal of*, vol.28, no.24, pp.3512,3518, Dec.15, 2010.

[22] Sugiyama, H.; Haruyama, S.; Nakagawa, M., "Brightness Control Methods for Illumination and Visible-Light Communication Systems," *Wireless and Mobile Communications, 2007. ICWMC '07. Third International Conference on*, vol., no., pp.78,78, 4-9 March 2007 PWM.

[23] Jong-Ho Yoo; Rimhwan Lee; Jun-Kyu Oh; Hyun-Wook Seo; Ju-Young Kim; Hyeon-Cheol Kim; Sung-Yoon Jung, "Demonstration of vehicular visible light communication based on LED headlamp," *Ubiquitous and Future Networks (ICUFN), 2013 Fifth International Conference on* , vol., no., pp.465,467, 2-5 July 2013.

[24] Lavric, A.; Popa, V.; Finis, I., "The design of a street lighting monitoring and control system," *Electrical and Power Engineering (EPE), 2012 International Conference and Exposition on*, vol., no., pp.314,317, 25-27 Oct. 2012.

[25] Alexandru, L.; Valentin, P., "Hardware design of a street lighting control system with vehicle and malfunction detection," *Advanced Topics in Electrical Engineering (ATEE), 2013 8th International Symposium on*, vol., no., pp.1,4, 23-25 May 2013.

[26] M. Hecht and A. Guida, "Delay Modulation, *Proceedings of the IEEE*, vol. 57, no. 7, pp. 1314-1316, July 1969.

[27] Berman, S. M., Greenhouse, D. S., Bailey, I. L., Clear, R. and Raasch, T. W., "Human electroretinogram responses to video displays, fluorescent lighting and other high frequency sources," Optometry and Vision Science 68:645–662, 1991.

[28] M. Rea, Illumination Engineering Society of North America (IESNA) Lighting Handbook, 9th ed., July 2000.

[29] The mobile communications handbook, 2nd edition, CRC Press LCC, 1999.

[30] Cailean, A.; Cagneau, B.; Chassagne, L.; Topsu, S.; Alayli, Y.; Dimian, M., "A robust system for visible light communication," *Wireless Vehicular Communications (WiVeC), 2013 IEEE 5th International Symposium on* , vol., no., pp.1,5, 2-3 June 2013 doi: 10.1109/wivec.2013.6698223.

[31] U.S. Department of Transportation. Vehicle Safety Communications Project Task 3 Final Report. http://www.ntis.gov/.

[32] A. J. C. Moreira, R. T. Valadas, and A. M. de Olveira Duarte, "Optical interference produced by artificial light," in Wireless Networks, 05-1997, Volume 3, Issue 2, pp 131-140.

[33] Hyuncheol Park and Barry, J.R, "Modulation analysis for wireless infrared communications," 1995. ICC '95 Seattle, 'Gateway to Globalization', IEEE International Conference on Communications, vol. 2, pp. 1182 - 1186, 1995.